Cancer Letters 633 (2025) 218011

Contents lists available at ScienceDirect

Cancer Letters

journal homepage: www.elsevier.com/locate/canlet

Original Articles

TP53-agnostic lethality through combined pan-HDAC and CDK inhibition in acute myeloid leukemia

Aurélien Pottier [a], Sujung Park [b,1], Yejin Lee [b], Francesca Liccardo [c], Haeun Yang [b], Jeonghye Park [b], Anne Lorant [a,2], Michael Schnekenburger [a,3], Davide Brusa [d], Vladimir Li [b], Sergio Valente [e], Antonello Mai [e], Sarah J. Skuli [f], Martin Carroll [f], Steffen Boettcher [g], Jean-Emmanuel Sarry [c], Claudia Cerella [a,4], Franck Morceau [a,*,5], Marc Diederich [b,**]

[a] Laboratoire de Biologie Moléculaire et Cellulaire du Cancer (LBMCC), 6A rue Nicolas-Ernest Barblé, L-1210, Luxembourg
[b] Research Institute of Pharmaceutical Sciences & Natural Products Research Institute, College of Pharmacy, Seoul National University, Seoul, 08826, Republic of Korea
[c] Equipe Labellisée LIGUE 2023, Team Oncometabolism and drug resistance in Acute Myeloid Leukemia, Cancer Research Center of Toulouse, 2 Av. Hubert Curien, 31100, Toulouse, France
[d] Flow Cytometry Platform, Université catholique de Louvain, B-1200, Bruxelles, Belgium
[e] Department of Drug Chemistry and Technologies, La Sapienza University of Rome, Piazzale Aldo Moro 5, 00185, Rome, Italy
[f] Division of Hematology & Oncology, Department of Medicine, University of Pennsylvania, Philadelphia, PA, 19104, USA
[g] Universitätsspital Zürich, Rämistrasse 100, CH-8091, Zürich, Switzerland

ARTICLE INFO

Keywords:
CAY10603
Cell cycle checkpoints
Dinaciclib
Epigenetics
MYC signaling
p21
SAHA

ABSTRACT

Tumor protein 53 (TP53)-mutated acute myeloid leukemia (AML) is characterized by poor outcomes and the quick development of treatment resistance. Here, we report that simultaneous inhibition of cyclin-dependent kinases (CDKs) and histone deacetylases (HDACs) with dinaciclib and CAY10603, respectively, eliminates the therapeutic response gap between TP53-mutant and TP53 wild-type AML. Biochemical profiling showed that CAY10603 is not only HDAC6-selective but also exhibits pan-HDAC activity similar to suberoylanilide hydroxamic acid, enabling dual targeting of transcriptional and cell cycle pathways. Across parental wild-type lines and isogenic TP53 mutants, the combination consistently suppressed clonogenic growth, induced caspase-dependent apoptosis, and downregulated key regulators such as CDK2, CDK4/6, and their cyclins, while restoring the CDK inhibitor CDKN1A/p21. In an orthotopic NSG mouse model, dinaciclib + CAY10603 significantly reduced leukemia burden and extended survival without adverse toxicity. By "normalizing" TP53-mutant AML to respond like its wild-type counterpart, this pan-HDAC/multi-CDK blockade offers a TP53-agnostic therapeutic option and warrants clinical evaluation as a strategy that remains effective regardless of baseline allelic status.

1. Introduction

Acute myeloid leukemia (AML) is a heterogeneous malignancy characterized by the clonal expansion of immature myeloid cells in the bone marrow and peripheral blood. Mutations in the tumor suppressor gene tumor protein (TP)53 occur in approximately 10 % of AML cases, leading to resistance to conventional chemotherapy and venetoclax/azacytidine combination therapy. The median overall survival (OS) is

* Corresponding author.
** Corresponding author. Department of Pharmacy, College of Pharmacy, Seoul National University, Gwanak-ro, Gwanak-gu, Seoul, 08826, Republic of Korea.
E-mail addresses: franck.morceau@lbmcc.lu (F. Morceau), marcdiederich@snu.ac.kr (M. Diederich).
[1] Catholic Hematology Hospital, Seoul St. Mary's Hospital, College of Medicine, The Catholic University of Korea, Seoul 06591, Republic of Korea.
[2] Luxembourg Centre for Systems Biomedicine, Bioinformatics Core, Roudeneck, 1, Boulevard du Jazz, L-4370 Esch-sur-Alzette, Luxembourg.
[3] Immune Endocrine Epigenetics Research Group, Department of Infection and Immunity, Luxembourg Institute of Health (LIH), 29 rue Henri Koch, L-4354 Esch-sur-Alzette, Luxembourg.
[4] Department of Cancer Research, Luxembourg Institute of Health (LIH), BAM Pavillon 2, 6A rue Nicolas-Ernest Barblé, L-1210 Luxembourg, Luxembourg.
[5] Department of Translational Medicine Operations Hub, Luxembourg Institute of Health (LIH), 1, rue Louis Rech, L-3555 Dudelange, Luxembourg. franck.morceau@lih.lu

https://doi.org/10.1016/j.canlet.2025.218011
Received 31 January 2025; Received in revised form 29 August 2025; Accepted 29 August 2025
Available online 1 September 2025

4–6 months, and a 2-year OS is less than 10 %. This poor outlook underscores the urgent need for effective therapeutic strategies for this high-risk patient population.

Multiple strategies have been proposed to target TP53-mutated AML ($AML^{TP53mut}$), including inhibitors of mouse double minute (MDM)2 homolog, B-cell lymphoma (BCL)2, TP53-MDM2-MDMX homolog interaction, cyclin-dependent kinase (CDK)9, and histone deacetylases (HDACs) in combination therapies [1–4]. Alternatively, TP53 reactivation and induction of massive apoptosis (PRIMA-1) and PRIMA-1Met (APR-246) are currently in advanced development, with several clinical trials in progress [5].

The TP53 gene is critical in preserving genomic stability by regulating cell cycle arrest, DNA repair, and apoptosis in response to cellular stress. Loss of TP53 function suppresses the expression of CDK inhibitor (CDKN)1A/p21 expression, an essential regulator of the G1/S checkpoint. Without CDKN1A/p21, CDK1, CDK2, and CDK4/6 activities cause hyperphosphorylation of the retinoblastoma (Rb) protein. This modification releases E2F transcription factors from the E2F/phospho-Rb complex, enabling E2F to drive the expression of genes vital for DNA synthesis and cell cycle progression. Therefore, inducing CDKN1A/p21 expression and/or targeting CDKs and cyclins (CCN) may reduce the proliferation and survival of $AML^{TP53mut}$ cells.

Interestingly, HDAC inhibitors (HDACi) have been shown to upregulate CDKN1A/p21 in various cell types [6,7]. Moreover, HDACis induce apoptosis and promote the accumulation of cells in the G0/G1 cell cycle phase. They also prevent MYC expression, which inhibits CDKN1A/p21 and CDKN2B/p15 expression, thus inhibiting cell proliferation [8].

Meanwhile, several pan-CDK inhibitors (CDKi) like flavopiridol (alvocidib) [9], AT7519 [10], and dinaciclib (SCH 727965) [11–14] have been developed and evaluated alone or in combination therapies in preclinical and clinical settings, including for hematological malignancies. Furthermore, combination therapies using specific CDK4/6 inhibitors (palbociclib, ribociclib, abemaciclib) are now the standard of care in first- and second-line metastatic settings, significantly improving progression-free and overall survival in breast cancer patients [15–18]. Additionally, the selective CDK9 inhibitor BAY1143572 (atuveciclib) has demonstrated promising results when combined with TRAIL in preclinical studies [19]. CDK9 regulates gene transcription by phosphorylating the C-terminal domain of RNA polymerase II, a process critical for transitioning into the elongation phase of transcription. Inhibiting CDK9 can downregulate short-lived anti-apoptotic proteins, which may be especially beneficial in AML.

In this study, we investigated the potential of dual targeting of CDKs and HDACs in both TP53 wild-type (AML^{TP53wt}) and, critically, $AML^{TP53mut}$ subtypes by using dinaciclib, a potent inhibitor of CDK1, CDK2, CDK5, and CDK9, and the pan-HDACi CAY10603. Although CAY10603 is recognized as a selective HDAC6 inhibitor [20], our data demonstrate that it inhibits additional HDAC isoforms, resulting in histone H3/H4 acetylation. Our current study shows notable similarities between CAY10603 and SAHA (suberoylanilide hydroxamic acid; vorinostat), supporting classifying CAY10603 as a pan-HDACi. These results refine our understanding of the CAY10603's mechanism of action and have implications for its use in research and therapeutic contexts.

Here, we examined the dual blockade of HDACs and CDKs with CAY10603 + dinaciclib across TP53 wild-type, TP53 mutant, and isogenic AML models. We also tested the regimen in an orthotopic xenograft of U-937-Luc cells in NSG mice. Strikingly, the combination "normalized" $AML^{TP53mut}$, eliminating the therapeutic sensitivity gap and producing cytotoxicity indistinguishable from that in AML^{TP53wt} cells. Mechanistically, CAY10603's newly defined pan-HDAC activity cooperated with dinaciclib's multi-CDK inhibition to halt cell cycle progression (via suppression of CDK2, CDK4/6, and their cyclins, and upregulation of CDKN1A/p21) and to trigger caspase-dependent apoptosis. In vivo, this resulted in a significant reduction in leukemic burden and prolonged survival without adverse toxicity. Overall, our findings position pan-HDAC/multi-CDK co-inhibition as a TP53-agnostic therapeutic strategy capable of counteracting the survival advantage conferred by mutant TP53 and of maintaining efficacy even as TP53 status evolves under treatment pressure.

2. Material and Methods

A detailed Material and Methods section is provided as a supplementary document.

2.1. Ethical considerations and experimental protocols

The Supplementary Material and Methods detail ethical considerations, experimental protocols, cell lines, reagents, antibodies, and data analysis methods. Cell lines are described in Table S1.

2.2. Healthy blood samples

$CD34^+$ hematopoietic stem and progenitor cells HSPCs were purified as follows: mononuclear cells were collected using Ficoll® (GE Healthcare, Roosendaal, The Netherlands) density gradient medium. Next, $CD34^+$ cells were selected by magnetic cell sorting in accordance with the manufacturer's instructions (Miltenyi Biotec, Utrecht, The Netherlands). The $CD34^+$ cells were cultured under serum-free conditions in Stem Line Medium II (Sigma-Aldrich, St. Louis, MO, USA) supplemented with L-glutamine, penicillin/streptomycin/amphotericin B (Lonza, Basel, Switzerland). Peripheral blood mononuclear cells (PBMCs) were isolated and cultivated as previously described [21,22]. Additional information on the sources, authentication, and culture conditions of all cell models used in this study is provided in the Supplementary Material and Methods.

2.3. In vivo studies

All animal experiments were conducted in compliance with the guidelines of the Institute of Animal Care and Use Committee (IACUC) at Seoul National University, Seoul, South Korea. The study protocol was approved by the IACUC Ethics Committee (SNU-220704-6-3 and SNU-241112-4). A detailed description of the in vivo studies is available in the Supplementary Material and Methods.

2.4. Statistical analysis

Details on data representation and statistical tests are provided in the figure legends. Statistical analyses were performed using Prism 10.0 or R version 4.2.0. The threshold for statistical significance was set at $p < 0.05$. Appropriate adjustments were made to account for multiple comparisons.

3. Results

3.1. High variant allele frequency of TP53 mutations impairs AML patient survival

To highlight the aggressive nature of $AML^{TP53mut}$, we categorized patients included in the BeatAML2 cohort [23] by variant allele frequency (VAF) of TP53 mutations and analyzed the impact on survival. From an initial cohort of 55 patients who had matched TP53 VAF and overall survival (OS) data, the impact of TP53 mutation burden on OS was investigated in patients' samples exhibiting high and low TP53 VAF (25th and 75th percentiles of TP53 VAF values; $N = 28$). This study revealed that individuals with a high VAF had significantly shorter survival than those with low VAF (Fig. 1A). This finding suggests that a higher mutation burden, reflecting the proportion of tumor cells harboring TP53 mutations, correlates with poorer prognosis. Moreover, in Cox proportional hazards models, start-stop gain/loss variants were

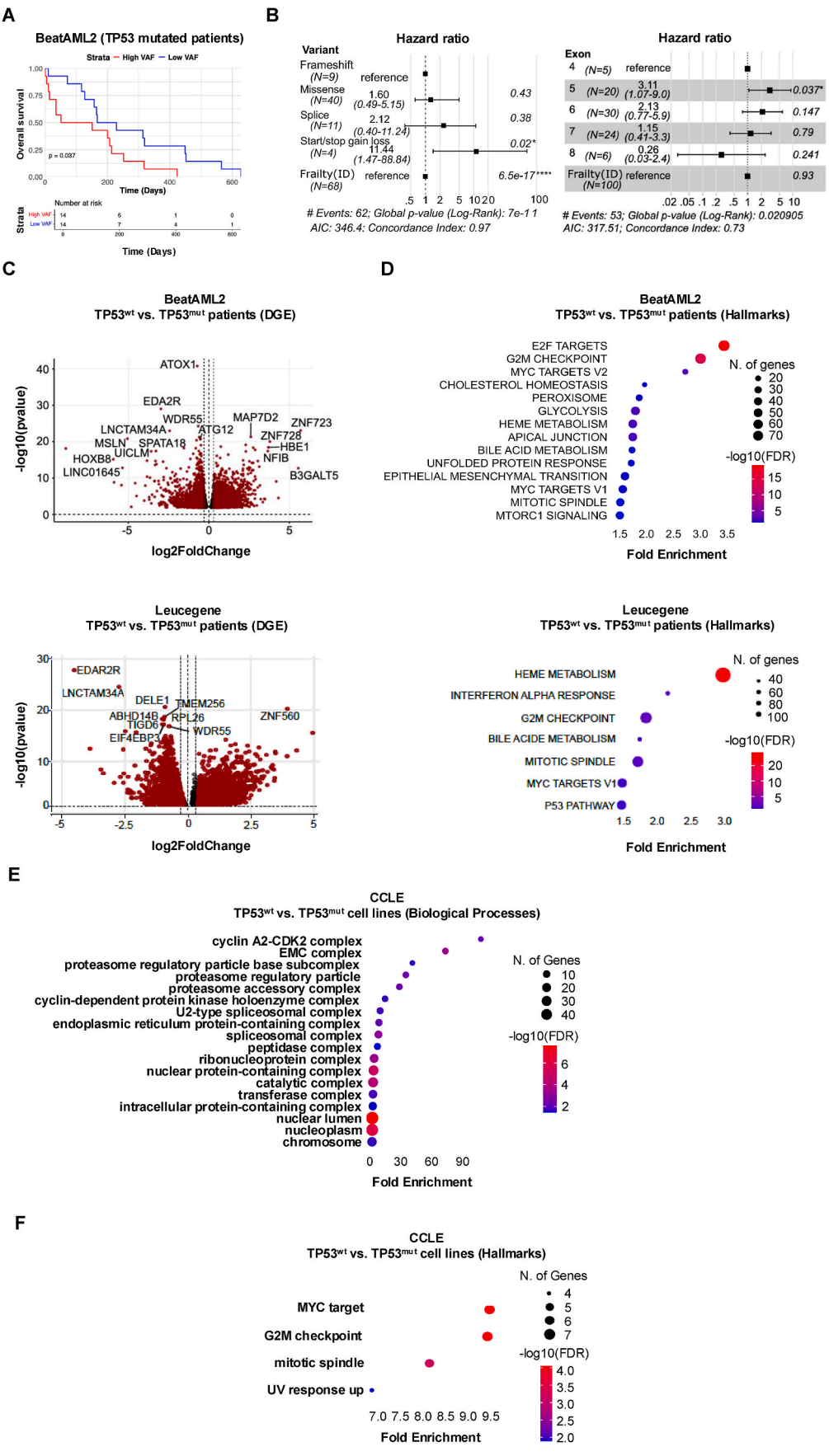

(caption on next page)

Fig. 1. Differential Gene Dependency and Pathway Enrichment Analyses reveal Key Vulnerabilities in TP53-mutated AML. **A.** Kaplan-Meier survival curves comparing the overall survival between patients with high and low TP53 variant allele frequency (VAF) classified by the 1st and 4th quartiles of VAF in the BeatAML2 cohort (N = 28). Patients with high VAF (red) had significantly shorter survival times than those with low VAF (blue): 101 vs. 197.5 days, respectively. Statistical significance was assessed using the log-rank test. **B.** Cox proportional hazard ratio analyses for TP53 variant classifications (left) and specific exons (right) in BeatAML2 patients. The hazard ratios and 95 % confidence intervals illustrate the risk associated with different TP53 mutation categories. **C.** Volcano plot displaying differentially expressed genes between AML^{TP53wt} and $AML^{TP53mut}$ patients from the BeatAML2 or Leucegene cohort. **D.** Hallmark pathways enrichment analysis of differentially expressed genes in $AML^{TP53mut}$ patients from the BeatAML2 or Leucegene cohort, performed using a hypergeometric test and corrected for multiple comparisons with the Benjamini-Hochberg (BH) method, applying a significance threshold of false discovery rate (FDR) < 0.05. Strata: stratification. **E-F.** Pathway enrichment analysis of genes showing significant differential effects on proliferation in $AML^{TP53mut}$ vs AML^{TP53wt} cell lines, as identified by CRISPR screens, based on gene ontology Biological Process terms (**E**) and hallmark pathways (**F**). This analysis used a hypergeometric test with a Benjamini-Hochberg correction for multiple comparisons, applying a significance threshold of false discovery rate (FDR) < 0.05. (For interpretation of the references to color in this figure legend, the reader is referred to the Web version of this article.)

significantly associated with an approximately 11-fold increase in the hazard of death (Fig. 1B). However, the significant frailty term indicates the presence of additional, unmeasured factors influencing the observed variability in OS. Notably, mutations in exon 5, essential for TP53's DNA-binding function, were linked to a 3-fold increase in the hazard of death. The strong predictive performance of these models, evidenced by concordance indexes of 0.97 and 0.73, underscores their utility for risk stratification (Fig. 1B).

3.2. Key regulators of cell cycle progression are deregulated in $AML^{TP53mut}$ patients

The significant impact of TP53 mutations on patient survival questions the underlying biological mechanisms driving disease aggressiveness. To understand how TP53 genomic alterations contribute to AML progression and identify actionable therapeutic targets, we analyzed the BeatAML2 and Leucegene patient cohorts [24–28]. This study aimed to uncover a mechanistic link between poor clinical outcomes and specific molecular defects, which could reveal vulnerabilities to be exploited for pharmacological targeting.

A comparative analysis of $AML^{TP53mut}$ and AML^{TP53wt} in the BeatAML2 and Leucegene cohorts revealed a significant enrichment of E2F, MYC targets, and G2M checkpoint genes, suggesting activation of pathways that drive cell cycle progression at both the G1/S and G2/M transitions (Fig. 1C and D). Cyclins and CDKs govern these processes, with the G2M checkpoint primarily regulated by the cyclin A/B–CDK1 complex and the G1/S transition mediated by cyclin D-CDK4/6 and cyclin E-CDK2, all of which are modulated by E2F factors. Notably, a comparative differential gene expression analysis of the E2F family genes (E2F1 to E2F8) in BeatAML2, Leucegene, and TCGA LAML cohorts found that E2F2 was significantly upregulated across all datasets, with the strongest differential expression seen in the Leucegene cohort (Log2FC = 1.56, padj = 9.24E-11; Table S2). Correlation studies between mRNA and proteomic expression levels of E2F family genes confirmed gene expression levels as reliable indicators for protein abundance, with E2F2 (Rs: 0.84) and E2F5 (Rs: 0.70) showing the strongest correlations (Table S3; [29]).

To identify genes with a functional impact on proliferation, we performed a differential dependency analysis using CRISPR gene effect data from 16 AML cell lines (Table S4). This approach identified 88 genes whose knockdown significantly inhibited proliferation in $AML^{TP53mut}$ cells compared to AML^{TP53wt} cells (Table S5). These genes were enriched in gene ontology (GO) categories involving the cyclin A2-CDK2 complex (Biological Processes; Fig. 1E), MYC targets, and the G2M checkpoint (Hallmarks; Fig. 1F).

3.3. CAY10603 displays pan-HDACi activity comparable to SAHA

Since HDACis offer a promising therapeutic approach by targeting the cell cycle control, we used the HDACi CAY10603. Even though CAY10603 is described as a selective HDAC6 inhibitor, the results of the present analysis led us to question this designation. First, an *in vitro* comparison of CAY10603 and SAHA showed that CAY10603 inhibited all tested HDACs similarly to SAHA. Second, all half-maximal inhibitory concentrations (IC_{50}) values for CAY10603 were lower than those for the pan-HDACi SAHA (Table S6), indicating that CAY10603 targets the same HDACs as SAHA *in vitro*, even more potently. Finally, CAY10603 induced acetylation of α-tubulin but also histone H3/H4, which is not a substrate of HDAC6, in HL-60 and U-937 cells, mirroring the effects of SAHA (Fig. 2A–C). These findings suggest that CAY10603 is not a selective HDAC6 inhibitor, underscoring the need to reexamine its selectivity profile and therapeutic potential.

3.4. CAY10603 and SAHA reduce $AML^{TP53mut}$ cell viability

Next, we hypothesized that the modulation of oncogenic drivers by CAY10603 primes AML cells for apoptosis. The HDACi treatment (1 μM) significantly impacted the cell cycle distribution of $AML^{TP53mut}$ cells, with a notable accumulation of HL-60 cells in the G1 phase and U-937 cells in the G2 phase. Both cell lines displayed a very strong reduction in the S phase (Fig. 3A). These results suggest that the HDACi disrupts cell cycle progression by modulating key regulators such as CDKN1A/p21, cyclins, and CDKs but also induces extensive apoptosis. These findings underscore the potent anti-leukemic activity of this HDACi in $AML^{TP53mut}$ cells.

We next compared the impact of CAY10603 and SAHA on the $AML^{TP53mut}$ cell lines HL-60, U-937, HEL, and KG-1, as well as the AML^{TP53wt} cell lines OCI-AML-3 and MV4-11. Both HDACis significantly, though differentially, reduced cell viability in all cell lines in a time- and concentration-dependent manner (Fig. 3B, Fig. S1). Notably, while both HDACi affected AML^{TP53wt} cells, they also reduced the viability of $AML^{TP53mut}$ cells in the same concentration range (1–4 μM). Interestingly, CAY10603 showed lower IC_{50} values than SAHA at 48 h (Table S7). Results were validated through colony formation assays (CFAs) in various AML cell lines (Fig. S2). CAY10603 (2 μM) and SAHA (2 μM) induced apoptosis in HL-60 and U-937 cells, as indicated by the cleavage of procaspases-3 and -9 and poly (ADP-ribose) polymerase (PARP)-1 at 24 h (Fig. 3C).

To validate in vivo efficacy, NSG mice were xenografted with TP53-mutated U-937-Luc cells. Bioluminescence imaging demonstrated that CAY10603 exerted a significantly stronger effect on $AML^{TP53mut}$ cell viability than SAHA for the same concentration (40 mg/kg) (Fig. 3D–F). Importantly, CAY10603 did not impair the viability of healthy PBMCs or $CD34^{+}$ hematopoietic stem and progenitor cells (Fig. 3G and H), underlining its excellent differential toxicity.

CAY10603 and SAHA reduce the $AML^{TP53mut}$ cell viability and induce cell death both *in vitro* and in vivo, underscoring their therapeutic potential. Notably, these inhibitors also reduce cell viability in other AML lines irrespective of TP53 status; however, their significance in the TP53-mutated context is essential, considering the dismal survival associated with TP53-mutated AML. Any agent that remains effective in this setting addresses an urgent clinical need.

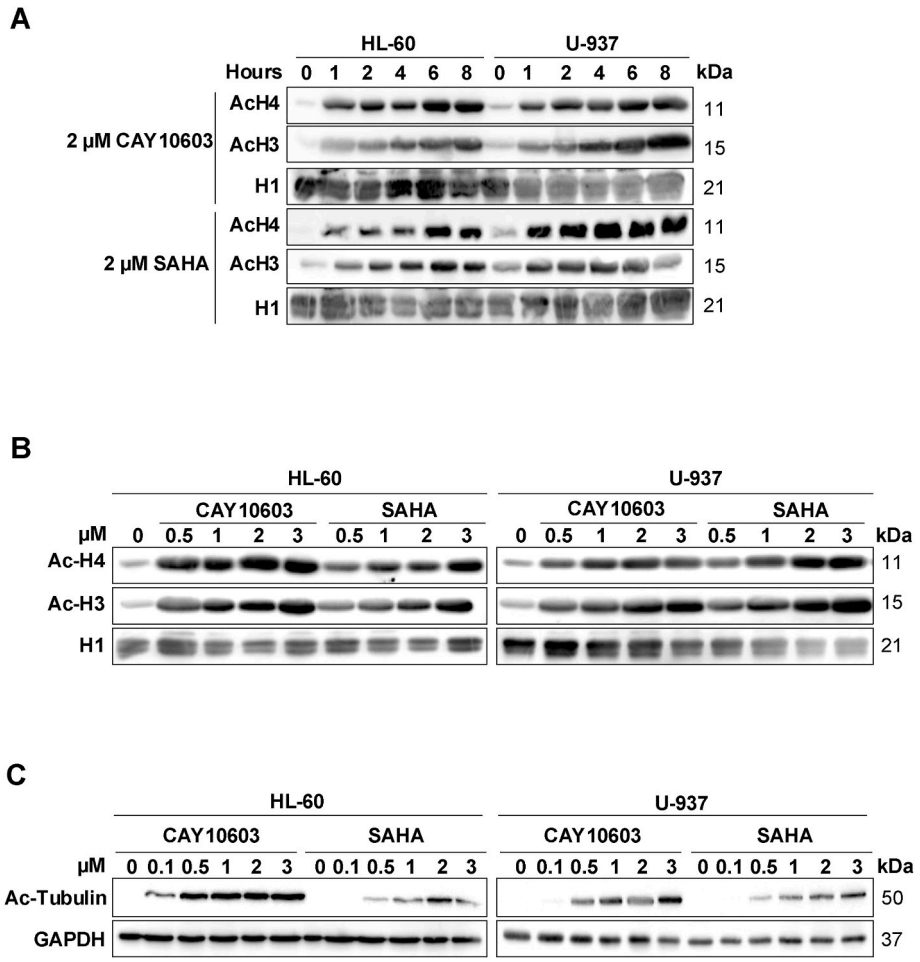

Fig. 2. Histone and Tubulin Acetylation Triggered by CAY10603 and SAHA. **A-C.** Western blot analyses showing the effects of CAY10603 and SAHA on the acetylation of histone H4 (Ac-H4) and H3 (Ac-H3) in HL-60 and U-937 cells, according to the indicated treatment times **(A)** and concentrations **(B)**. **C.** Western blot analysis of acetylated tubulin at the specified treatment concentrations. Histone H1 and GAPDH were used as loading controls. Blots are representative of three independent experiments.

3.5. HDACi modulate gene expression of key cell cycle regulators in AML^{TP53mut} cell lines

To better understand the molecular mechanisms, we conducted RNA-seq analyses to investigate the impact of HDACi on the expression of key cell pathways critical to AML^{TP53mut} cell survival.

HL-60 and U-937 cells were treated with 2 µM CAY10603 or SAHA for 8 h. RNA-seq analyses revealed a substantial overlap and strong correlation between CAY10603- and SAHA-treated samples in both cell lines (Fig. 4A–C), indicating similar effects on gene expression. CAY10603 and SAHA treatments in HL-60 and U-937 cells significantly downregulated MYC and E2F target genes, as well as G2M checkpoint regulators, while activating the TP53 pathway (Fig. 4D). Additionally, transcription factors MYC and several members of the E2F family (E2F3, E2F5, and E2F6) were markedly reduced in both cell lines (Fig. 4E). Of particular note, the expression of the cell cycle checkpoint regulators CDKN1A/p21, CDKN2B/p15 and CDKN2D/p19 mRNA was upregulated, whereas transcripts for CDK6, CCN-D, -A, and -B were downregulated in HL-60 and U-937 cells (Fig. 4F). These results suggest that CAY10603 and SAHA concurrently activate the p21/CCN-CDK/E2F pathway, partially reversing the transcriptional profile previously observed in AML^{TP53mut} patients (Fig. 1D).

Western blot analyses showed that MYC expression decreased as early as 2 h after CAY10603 (2 µM) and SAHA (2 µM) treatment in HL-60 and U-937 cells, reaching near-total inhibition at 24 h. This inhibitory effect was more pronounced in CAY10603-treated cells and in U-937 cells. In line with this reduction in MYC expression, acetylation of MYC at lysine residues K148/K323 was more prominent in CAY10603-treated cells compared to SAHA and more so in U-937 cells, indicating CAY10603's ability to modulate the acetylation of non-histone proteins (Fig. 5A).

As expected, p21 protein expression was constitutively present in AML^{TP53wt} cells but absent in AML^{TP53mut} cells, where its level was inversely correlated with E2F1 expression (Fig. 5B). HDACi restored p21 expression in AML^{TP53mut} cells, while E2F1 expression was markedly diminished. Additionally, the TP53-independent p15 expression was also elevated (Fig. 5C). In agreement with the RNA-seq data, as well as with MYC and E2F1 modulation, the expression of CDK4/6 and the CDK2 partners CCNE1 and CCNA2 decreased in HDACi-treated cells (Fig. 5D). Furthermore, HDACi decreased Rb levels at 24 h, while S807/811 residues phosphorylation remained stable in CAY10603 (2 µM)- and SAHA (2 µM)-treated HL-60 cells with a stronger effect for CAY10603 (Fig. 5E). This finding implies ongoing CDK activity and suggests that HDAC inhibition alone may be insufficient to suppress the cell cycle machinery fully.

3.6. Dinaciclib induces cell death in AML^{TP53mut} cell lines

The ability of CAY10603 to disrupt cell cycle progression by restoring negative regulators such as CDKN1A/p21 and downregulating oncogenic drivers like MYC and E2F1 creates a synergistic opportunity for combination therapy. Moreover, the addition of a CDK inhibitor may

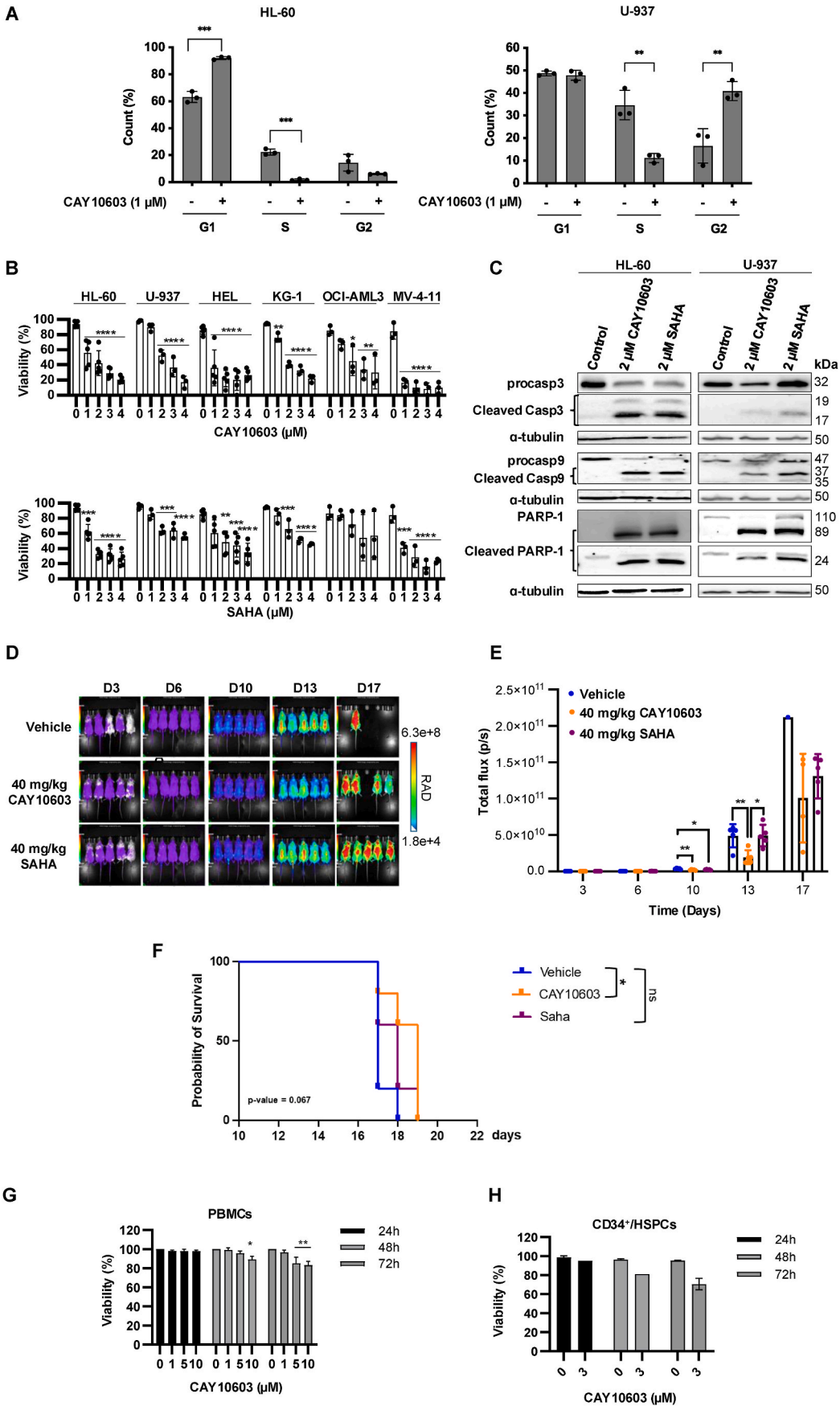

(caption on next page)

Fig. 3. Effect of HDAC inhibitors on AML cell viability *in vitro* and in vivo. **A.** Cell cycle analysis in 24 h CAY10603-treated $AML^{TP53mut}$ cell lines. **B.** Viability in 48 h CAY10603 or SAHA-treated $AML^{TP53mut}$ (HL-60, HEL, KG-1, U-937) and AML^{TP53wt} (MV4-11, OCI-AML-3) cell lines treated with increasing concentrations of the indicated compounds. **C.** Western blot analysis of caspase 9 (Casp9), caspase 3 (Casp3), and PARP-1 cleavage of HL-60 and U-937 cells treated for 24 h with 2 μM CAY10603 or 2 μM SAHA. α-tubulin was used as a loading control. Blots are representative of three independent experiments. **D-E.** Effect of HDACi in a U-937-Luc xenograft study (N = 5 mice/group). **D.** Bioluminescence imaging of U-937-Luc cells after tail vein injection. CAY10603 or SAHA (40 mg/kg; intraperitoneal injection; 5 times a week) were administered. **E.** Quantification of the total bioluminescent flux over time. **F.** Kaplan-Meier survival analysis. **G-H.** Assessment of cell viability in healthy cell models cultured for up to 72 h: **(G)** peripheral blood mononuclear cells (PBMCs) treated with 1, 5, and 10 μM CAY10603; **(H)** $CD34^+$ hematopoietic stem and progenitor cells (HSPCs) treated with 3 μM CAY10603. Data represent the mean ± SD of at least 3 (2 for $CD34^+$ cells) independent experiments. P values were determined by unpaired two-tailed *t*-test (**A**); one-way ANOVA with Dunnett's multiple comparison test (**B,G**); one-way ANOVA with Tukey's multiple comparison test (**E**) and Log-rank test **(F)**. Significance levels are indicated as *p ≤ 0.05, **p ≤ 0.01, ***p ≤ 0.001, ****p ≤ 0.0001.

disrupt Rb phosphorylation, leading to enhanced cell cycle arrest and apoptosis in $AML^{TP53mut}$ cells. Dinaciclib, a potent CDK inhibitor targeting CDK1, CDK2, CDK5, and CDK9, could complement the effects of CAY10603 by further suppressing key cell cycle and survival pathways.

Dinaciclib significantly reduced cell viability at 8–16 nM in AML^{TP53wt} and $AML^{TP53mut}$ cell lines (Fig. 6A). At 48 h, IC_{50} values were 13 nM for HL-60 cells and 9 nM for U-937 cells (Table S7). Notably, the clonogenic ability was highly impaired with a reduction in colony size and numbers at reduced concentrations (Fig. 6B, Fig. S3).

To further explore these effects, we compared the impact of dinaciclib and CAY10603 over time in HL-60 and U-937 cells by examining the expression of anti-apoptotic proteins (BCL-2, MCL-1) and the pro-apoptotic protein NOXA. Western blot analyses indicated that MCL-1 expression was elevated at early time points in CAY10603 (2 μM)-treated cells. In contrast, dinaciclib (13 and 9 nM, respectively) down-regulated MCL-1 at early time points in HL-60 cells and fully suppressed MCL-1 in U-937 cells at its IC_{50} (Fig. 6C). Both drugs reduced BCL-2 expression in HL-60 and U-937 cells. Meanwhile, Noxa was strongly overexpressed under CAY10603 treatment and remained unchanged with dinaciclib.

In addition, regulators of cell cycle progression (CCNA2, CCNE1, E2F1, and MYC) were downregulated in HL-60 and U-937 cells (Fig. 6D). Interestingly, CDK4, a non-selective target of dinaciclib, was also diminished.

3.7. A combination of CAY10603 with dinaciclib results in AML cytotoxicity

The rationale for combining CAY10603 with dinaciclib stems from their complementary mechanisms of action, which result in the down-regulation of MCL-1 and MYC. Meanwhile, CAY10603 induces apoptosis via HDAC inhibition and upregulates p21 and p15 in $AML^{TP53mut}$ cells.

Treating cells with 0.5, 1, and 2 μM CAY10603 combined with 6 or 9 nM dinaciclib significantly decreased the viability and number of living HL-60 and U-937 cells at 24 h compared to individual treatments (Fig. 7A and B). The effect was more pronounced in U-937 cells, where most combinations caused a greater reduction in viability, indicating increased sensitivity to the combination. To assess potential synergy, the combination index (CI) was calculated using the Chou-Talalay method. In HL-60 cells, no synergy was observed for viability, as all CI values were above 1. However, synergistic inhibition of proliferation was observed at the lowest concentrations tested. Notably, the combination of 0.5 μM CAY10603 with 6 or 9 nM dinaciclib yielded a CI of 0.6, with both drugs below their IC_{50}, indicating a strong cooperative effect at low doses (Fig. 7A). In U-937 cells, the combination showed stronger synergy, with CI values below 1 for both viability and proliferation across multiple dose combinations, including sub-IC_{50} concentrations (Fig. 7B). Interestingly, this effect was reached in combination treatments with lower concentrations than IC_{50}s and was confirmed by CFAs (Fig. S4).

To determine whether the dual CDK/HDAC strategy is affected by TP53 genotype or mutation burden, we used isogenic derivatives of the parental MOLM-13 (WT-TP53, BCL-2-high/MCL-1-low) and MOLM-14 ($TP53^{wt}$, MCL-1-high) backgrounds. Annexin-V/PI assays were performed 48 h after exposure to CAY10603 (500 nM), dinaciclib (1 or 2 nM), or their combination. CAY10603 reduced viability by 30–45 % in all clones, regardless of TP53 status; dinaciclib alone caused ≤25 % loss at 1 nM and approximately 35 % at 2 nM. In MOLM-13 cells, only the combination treatment significantly decreased viability compared to control in both $TP53^{wt}$ and mutated isogenic cell lines. The combination further decreased viability in TP53 KO MOLM-13 cells compared to single agents. In contrast, in MOLM-14 cells, CAY10603 alone was sufficient to strongly reduce viability. Viability reduction was greatest in the MCL-1-high MOLM-14 background (around 70 %) and least noticeable in BCL-2-dominant MOLM-13 (around 50 %). These data suggest that CAY10603 plus dinaciclib is effective regardless of TP53 mutation type or allelic state. Meanwhile, the strength of the response is influenced more by the cell's reliance on short-lived anti-apoptotic proteins than by TP53 function itself (Fig. 7C).

We then analyzed the effect of the combination on apoptosis and cell cycle regulator proteins. HL-60 and U-937 cells were treated (8 h) with 2 μM CAY10603 and 9–13 nM dinaciclib, and Western blot analyses revealed that the combination inhibited CDK6 expression. In contrast, individual treatments induced only a slight decrease at this time point. The combination also more effectively activated caspase-9 and PARP-1, as reflected by the cleavage of pro-caspases and PARP-1. We next assessed p21 expression at 24 h and showed that p21 was restored in CAY10603-treated cells but not in dinaciclib-treated cells. In co-treated HL-60 cells, p21 expression persisted, albeit at a lower level, likely due to heightened cytotoxicity, which was even more pronounced in U-937 cells (Fig. 8A). Moreover, the analysis of the Rb phosphorylation status at S807/811 ($Rb^{S807/811}$) in HL-60 cells showed that the combination CAY10603/dinaciclib triggered a decrease in $Rb^{S807/811}$ phosphorylation at 8 h compared to the control cells. Furthermore, in the combined treatment, dinaciclib prevented the CAY10603-induced stabilization of the phosphorylation at 24 h (Fig. 8B).

To further confirm that the observed cell death was apoptotic and caspase-dependent, we performed Annexin V-FITC/DAPI staining followed by flow cytometry analysis in HL-60 and U-937 cells treated with CAY10603, dinaciclib, or their combination (Fig. S5). In U-937 cells, combination treatments significantly increased the percentage of total Annexin V-positive cells compared to single-agent treatments and decreased the proportion of double-negative (viable) cells (Fig. S5 A-C). Conversely, in HL-60 cells, although both CAY10603 and dinaciclib induced apoptosis, the combination treatment did not further increase Annexin V positivity beyond the levels seen with the single agents (Fig. S5 D-F). Notably, the pan-caspase inhibitor zVAD-FMK markedly reduced Annexin V positivity in both cell lines, confirming that the cytotoxic effects were mainly mediated through caspase-dependent apoptosis. Similarly, in MV411 and HEL cells treated with CAY10603, dinaciclib, or their combination, Annexin V-FITC/DAPI staining confirmed apoptosis as the primary cell death mechanism. Flow cytometry showed a clear shift toward the Annexin V-positive population with only a minimal increase in DAPI-only positive cells. This gating pattern indicates that the cytotoxicity observed was primarily due to apoptosis rather than necrosis (Fig. S6).

To quantify anti-leukemic activity in vivo, we established an orthotopic xenograft model by injecting 1×10^5 U-937-Luc cells intravenously into NSG mice, followed by randomization on day 3 into four treatment arms (n = 5 each): vehicle, CAY10603 40 mg/kg (i.p., 5 × week), dinaciclib 5 mg/kg (i.p., 1 × week), or the combination. Vehicle-

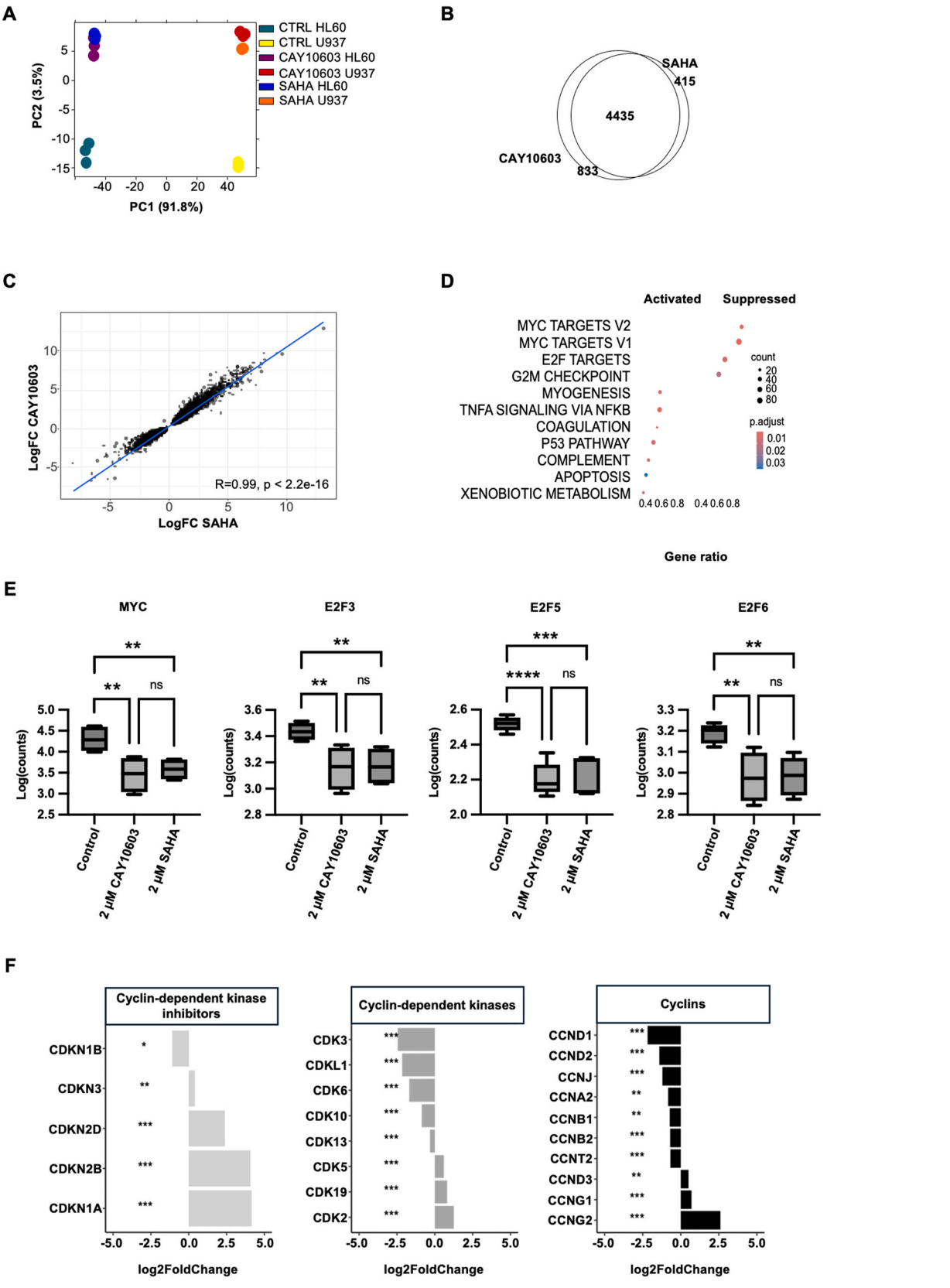

(caption on next page)

Fig. 4. Gene expression analysis in HL-60 and U-937 cell lines following treatment with CAY10603. **A.** Principal component (PC) analysis plot of the top 500 most variable genes, showing the separation of samples based on treatment conditions [2 μM CAY10603, 2 μM SAHA, and control (CTRL)] after 8 h. Each point represents a color-coded sample according to the treatment group and cell line (U-937 or HL-60). **B.** Venn diagram showing the overlap in differentially expressed genes between CAY10603 and SAHA treatments, with a high intersection indicating shared gene expression changes. **C.** Scatter plot comparing the log2 fold changes (LogFC) of differentially expressed genes between CAY10603 and SAHA treatments. Each point represents a gene, with a linear regression line (blue) showing a high correlation (Pearson R = 0.99, $p < 2.2e{-}16$). **D.** Gene set enrichment analysis (GSEA) plot showing the enrichment of differentially expressed genes across hallmark pathways in CAY10603-treated vs untreated cells. Significantly, enriched pathways are indicated with a false discovery rate (FDR) < 0.05. **E.** Differential expression analysis of MYC and E2F family genes. **F.** Differential expression analysis of cell cycle-related genes following CAY10603 treatment, categorized by cyclins (CCN), cyclin-dependent kinases (CDKs), and cyclin-dependent kinase inhibitors (CDKIs). Data represent the mean ± SD of 3 independent experiments. Statistical analysis of gene expression was performed using the BH method to control for FDR, with a significance threshold set at FDR <0.05 **(D, F)**; one-way ANOVA with Tukey's multiple comparison test **(E)**. Significance levels are indicated as follows: *$p \leq 0.05$, **$p \leq 0.01$, ***$p \leq 0.001$, ****$p \leq 0.0001$; ns: not significant. (For interpretation of the references to color in this figure legend, the reader is referred to the Web version of this article.)

treated mice exhibited exponential disease expansion, whereas single-agent CAY10603 or dinaciclib delayed but did not prevent progression. In contrast, the combination suppressed luminescence to near-baseline levels through day 18 and maintained a significant reduction versus vehicle at every subsequent time point (Fig. 8C and D). Kaplan–Meier analysis showed median survivals of 14 days for vehicle, 17 days for dinaciclib, 19 days for CAY10603, and 26 days for the combination. The dual regimen extended lifespan by 86 % relative to vehicle and by 37 % over the best single agent; log-rank testing yielded $P < 0.0001$ overall and $P < 0.01$ for all pairwise comparisons between the combination and each other group. Together, these data demonstrate that concomitant pan-HDAC and CDK inhibition produces a synergistic, durable suppression of systemic AML burden and markedly prolongs survival beyond either monotherapy in an aggressive orthotopic model (Fig. 8E).

These potent anti-leukemic effects were achieved without inducing hepatic or renal toxicity (Fig. S7). Moreover, in healthy C57BL/6 mice treated with the combination of CAY10603 and dinaciclib, the complete blood count analysis showed that neutrophil, eosinophil, basophil, and platelet counts remained within or close to the normal reference range (Fig. S8). Platelet levels were consistently maintained, and no cytopenia was observed in all treated groups. A transient reduction in circulating lymphocytes was observed, while monocyte levels recovered by both day 6 and day 14 post-treatment. The results showed that the combination treatment maintains steady-state hematopoiesis and is well tolerated.

4. Discussion

Despite a growing range of experimental treatments, long-lasting therapeutic control of $AML^{TP53mut}$ remains challenging. Venetoclax (VEN) combined with hypomethylating agents (HMAs) shows promising initial remissions, with Complete Remission/Complete Remission with incomplete count recovery (CR/Cri) of approximately 47–56 %, but median OS stalls at 7–7.2 months [30,31]; resistance often develops through compensatory MCL-1 upregulation. Antibody-based macrophage engagement with magrolimab plus azacitidine achieves CR/CRi around 40 % and median OS about 9.8 months, but its confirmatory phase III trial was recently stopped for futility [32,33]. Early-phase TIM-3 blockade with sabatolimab produces modest, sometimes lasting responses (overall response rate 20 % in high-risk myelodysplastic syndrome (MDS)/AML; median response duration 21.5 months) and is still evolving [34,35], while checkpoint inhibitor combinations (e.g., nivolumab with azacitidine) yield objective response rate (ORR) up to 33 % with median OS near 6 months [36]. TP53-reactivating strategies like eprenetapopt with azacitidine reached only a 17 % CR rate and did not succeed in a key phase III trial [37]. Bispecific T-cell engagers (flotetuzumab) produce transient CR/CRi in 47 % with OS around 4 months [38].

In this context, our data present the first dual epigenetic and cell-cycle blockade, pan-HDAC inhibition by CAY10603 combined with multi-CDK inhibition by dinaciclib. This combination simultaneously downregulates MCL-1 transcription (via CDK9 inhibition) and re-primes AML cells for apoptosis, thus counteracting resistance pathways limiting VEN, magrolimab, and APR-246-based therapies [39]. To our knowledge, no ongoing trial pairs any HDAC inhibitor with a CDK inhibitor, highlighting our approach's novelty and translational importance.

Dysregulation of the cell cycle is a key characteristic of cancer and often occurs alongside TP53 mutations [40]. Comparative gene expression analysis revealed a significant enrichment of G2M, MYC, and E2F target genes in $AML^{TP53mut}$ patients, indicating the activation of pathways critical for cell cycle progression at G1/S and G2/M transitions. Comprehensive differential gene expression analysis across multiple AML patient blast cohorts revealed consistent upregulation of *E2F* gene family members, with *E2F2* modulation conserved across all groups. Notably, within the *E2F* family, mRNA expression levels predict corresponding protein abundance, with correlation values falling within or exceeding the average expected range (~0.5 for most proteins) [29].

Using CRISPR gene dependency data, we consistently identified 88 genes whose inhibition significantly reduced proliferation in $AML^{TP53mut}$ cells compared to AML^{TP53wt} cells. The enrichment of dependencies in the CCNA2-CDK2 complex and MYC target genes highlights the reliance of $AML^{TP53mut}$ cells on these pathways for survival.

HDACi treatment restored CDKN1A/p21 expression in $AML^{TP53mut}$ cells, suggesting alternative regulatory mechanisms independent of TP53 function, possibly through modulation of chromatin structure and transcription factor accessibility [41]. Indeed, previous studies reported enhanced histone H4 acetylation and RNA polymerase II enrichment at the CDKN1A/p21 promoter after HDACi treatment in leukemia cells [42]. CDKN1A/p21 can also be induced through TP53-independent mechanisms involving nuclear receptors [43]. Conversely, active TP53 may negatively influence the HDACi trichostatin A (TSA)-mediated induction of p21, as TSA strongly induced p21 expression in mutant cells but not in their wild-type counterparts [44].

Given the reliance of $AML^{TP53mut}$ cells on CDKs and the ability of HDACi to modulate the TP53 pathway and restore CDKN1A/p21 expression, we explored the therapeutic potential of dual CDK/HDAC inhibition. HDACi, including SAHA, have been shown to induce apoptosis and cause cell cycle arrest in AML cells [45]. Although CAY10603 is considered a selective HDAC6 inhibitor, our study demonstrated its potent pan-HDAC inhibitory activity and greater potency than SAHA in reducing $AML^{TP53mut}$ cell viability *in vitro* and in vivo.

Additionally, HDACi partially reversed the aberrant transcriptional profile of $AML^{TP53mut}$ cells by downregulating CDK4/6, CCND1/2, MYC, and E2F1. Intriguingly, CDK4/6 inhibition has been linked to Rb degradation and reduction of E2F activation in breast cancer cells [46]. TP53 has been reported to repress MYC transcription via histone deacetylation [47], and MYC suppresses the transcription of CDKN1A/p21 and CDKN2B/p15 genes [48]. CAY10603 and SAHA downregulated constitutive expression of MYC in AMLTP53mut cells in correlation with HDACi-mediated hyperacetylation of MYC at K143/K323, known to promote its proteasomal degradation [49]. Inhibiting the constitutive expression of MYC by CAY10603 and dinaciclib thus fosters the reactivation of CDKN1A/p21 and CDKN2B/p15 in the absence of functional TP53.

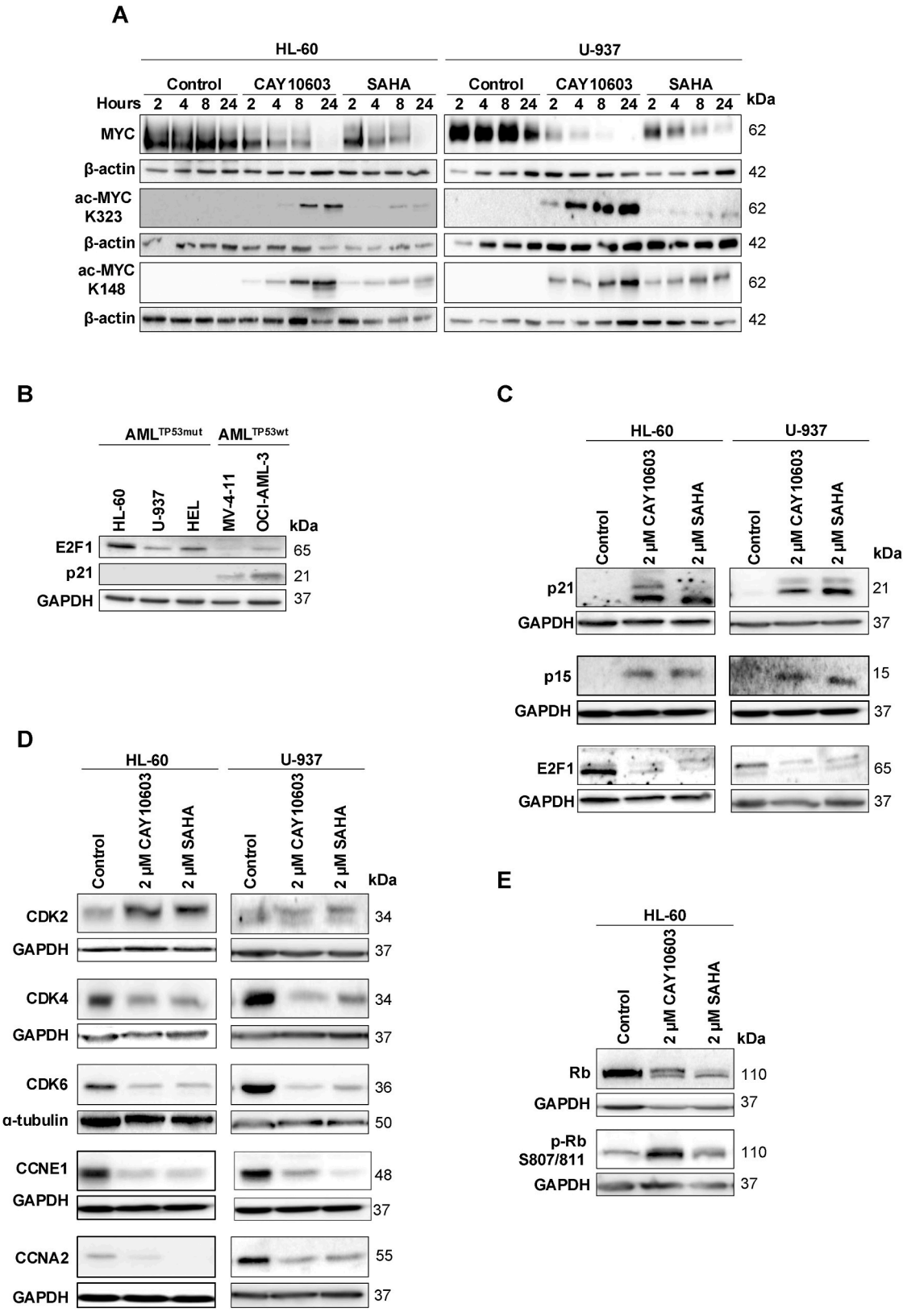

Fig. 5. Protein expression in HL-60 and U-937 cell lines following treatment with CAY10603 or SAHA. **A.** MYC and acetylated MYC (ac-MYC K323, K148) protein levels after treatment with 2 μM of the indicated compounds at the indicated time points. **B.** Western blot analysis of E2F1 and p21 protein levels in AML cell lines. **C-D.** Western blot analysis of **(C)** cyclin-dependent kinase (CDK) inhibitors and E2F1 and **(D)** cyclins (CCN) and their corresponding CDKs in HL-60 and U-937 cells treated with 2 μM of CAY10603 or SAHA for 24 h. Blots are representative of three independent experiments. **E.** Western blot analysis of total and phosphorylated retinoblastoma (p-RbS807/811) in HL-60 cells treated with 2 μM of CAY10603 or SAHA for 24 h. GAPDH and β-actin were used as internal loading controls. Immunoblot pictures represent at least three independent experiments.

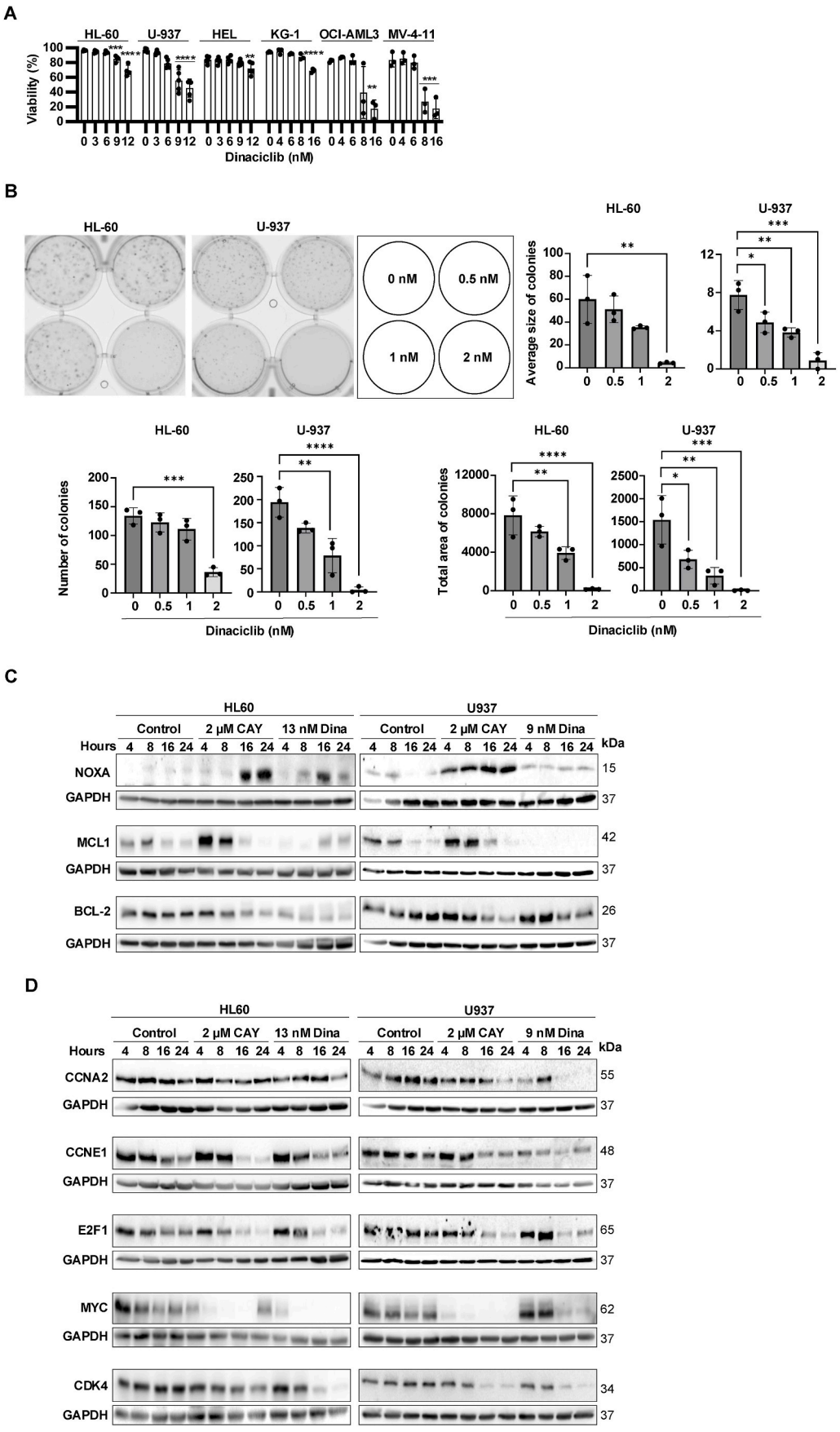

(caption on next page)

Fig. 6. Effect of CDK inhibitor Dinaciclib on viability and the cell cycle. **A.** Viability of AML^{TP53mut} (HL-60, HEL, KG-1, U-937) and AML^{TP53wt} (MV4-11, OCI-AML-3) cell lines treated with increasing concentrations of dinaciclib at 48 h. **B.** Effect of dinaciclib on colony formation capacity. Cells were pre-treated for 24 h before seeding. Representative images from three independent experiments after 10 days of incubation and corresponding quantification. **A-B.** Data represent the mean ± SD of at least 3 independent experiments. **C-D.** Western blot analysis in HL-60 and U-937 cells after treatment with 2 μM of CAY10603 (CAY) or 13 and 9 nM of dinaciclib (Dina), respectively. **C.** Anti-apoptotic proteins MCL-1 and BCL-2, pro-apoptotic protein NOXA, and **(D)** cell cycle-related proteins CCNA2, CCNE1, E2F1, MYC, and CDK4. P values were determined by one-way ANOVA with Dunnett's multiple comparison test. Significance levels are indicated as follows: *p ≤ 0.05, **p ≤ 0.01, ***p ≤ 0.001, ****p ≤ 0.0001. GAPDH serves as an internal loading control. Blots are representative of three independent experiments. Abbreviations: CAY: CAY10603; Dina, dinaciclib.

A screening of small molecule inhibitors targeting epigenetic and transcriptional regulators showed that the HDACi panobinostat and dinaciclib induced apoptosis in leukemic cells derived from genetically engineered, MLL–AF9–driven mouse AML models [42]. Nevertheless, in this specific murine model, the combination of panobinostat/dinaciclib did not produce an additive or synergic effect on cell viability. In contrast, our results showed that the CAY10603/dinaciclib combination significantly reduced U-937 AML^{TP53mut} cell viability *in vitro* and in vivo experiments.

Using the Chou–Talalay method, we found that the CAY10603 + dinaciclib combination exhibits dose-dependent synergy that is most pronounced at sub-IC_{50} concentrations and in TP53-mutant U-937 cells. In HL-60 cells, the combination displayed clear synergistic inhibition of proliferation at the lowest tested doses (0.5 μM CAY10603 + 6 or 9 nM dinaciclib; CI ≈ 0.6). In contrast, U-937 cells showed CI < 1 across multiple dose pairs for viability and proliferation, confirming a stronger cooperative effect. These data validate our use of the term "synergistic," highlight the therapeutic advantage of low-dose combinations, and reinforce the observation that the regimen neutralizes, but does not depend on, TP53 status for efficacy. Saidahmatov et al. [50] showed that a combination of SAHA and the selective CDK9 inhibitor NVP-2 produced a synergistic antileukemic effect in the AML^{TP53wt} MV-4-11 (AML FAB M5) cells. These cells express the MLL-AF4 fusion gene, are characterized by the t(4; 11) translocation, and carry an *FLT3*-ITD mutation. The specificities of individual cell models and their murine or human genetic backgrounds may influence responses to HDAC/CDK inhibitions and remain to be further investigated in the future.

MYC is a key driver of leukemic proliferation, yet its stability and activity are sensitive to lysine acetylation. p300/CBP-mediated acetylation at K148 and K323 can recruit ubiquitin ligases and accelerate proteasomal degradation, transforming MYC from an oncogenic activator into a short-lived, transcriptionally inactive form [51]. HDACi leverage this vulnerability; Nebbioso et al. showed that acetyl-K323 is a pharmacodynamic marker of HDACi response and coincides with TRAIL-mediated apoptosis in AML cells [52]. Our data expand this model by showing that dual pan-HDAC/CDK inhibition increases K148/K323 acetylation and suppresses MYC transcription, creating a double inhibition that disrupts the MYC gene-expression program and triggers cell cycle arrest. The paradox of "more acetylated MYC but less MYC activity" is thus explained: acetyl-MYC is quickly targeted for degradation and cannot engage its target promoters. This mechanistic convergence accounts for the sharp decrease in S-phase entry and the priming of cells for later apoptosis. Although acetylation has been reported to stabilize MYC in certain contexts, recent structure-function studies by Hurd et al. mapped distinct lysine clusters that can exert gene-specific effects on MYC biology [53]. Our finding that K148/K323 acetylation accompanies MYC loss and growth arrest highlights the importance of the context in these modifications and supports further investigation of acetyl-lysine-specific MYC inhibitors or degraders as rational partners for HDAC/CDK blockade.

Combining CAY10603 with dinaciclib significantly reduced cell viability and improved survival outcomes in vivo compared with single-agent treatments. Annexin V–FITC/DAPI quantification studies confirm that caspase-dependent apoptosis is the primary mode of cell death induced by the CAY10603 + dinaciclib combination. In TP53-mutant U-937 cells, the combination significantly increased the proportion of Annexin V-positive cells compared to either monotherapy, aligning with the synergy observed in viability assays; the near-complete rescue by the pan-caspase inhibitor zVAD-FMK highlights a classic apoptotic mechanism. In TP53-null HL-60 cells, each single agent already caused high Annexin V positivity and zVAD-FMK blocked cell death, indicating reliance on caspases. Similar Annexin V shifts in HEL and MV4-11 lines extend this finding across additional genetic backgrounds. Overall, these data demonstrate that the combined anti-leukemic effect results from convergent activation of the intrinsic apoptotic pathway rather than necrosis or off-target toxicity, and that this apoptosis trigger functions independently of TP53 status, consistent with the "normalizing" effect of the "double-hit" treatment. Dual inhibition effectively led to the downregulation of anti-apoptotic proteins (BCL-2, MCL-1) and upregulation of the pro-apoptotic protein NOXA, culminating in enhanced apoptosis in AML^{TP53mut} cells. Our study demonstrates that administering CAY10603 with dinaciclib exerts potent anti-leukemic effects through complementary mechanisms, blocking cell cycle progression and promoting apoptosis by targeting CDK2, CDK4/6, and their associated cyclins.

The phosphorylation status of the Rb protein plays a complex role in cell cycle regulation. Rb$^{S807/811}$ phosphorylation is a marker of hyperphosphorylation, which prevents apoptosis and is correlated with E2F activity, whereas hypophosphorylation leads to apoptosis [41,54–57]. Moreover, Rb$^{S807/811}$ is phosphorylated by the CCNC-CDK3 complex, which was reported to promote the G0/G1 phase transition [58]. CAY10603 inhibited CDK3 mRNA and induced an accumulation of HL-60 cells in the G1 phase at 24 h. HDACi induced Rb$^{S807/811}$phosphorylation at 24 h, suggesting ongoing CDK activity in HDACi-treated HL-60 cells. Nevertheless, the E2F family of transcription factors, including the E2F1 protein, was downregulated in AML^{TP53mut} cells by CAY10603 and dinaciclib, suggesting that E2F downregulation is at least partially independent of Rb phosphorylation status. The combination of CAY10603/dinaciclib prevented the stabilization of Rb$^{S807/811}$ phosphorylation, decreasing the hyperphosphorylated form of Rb in HL-60 cells. Dinaciclib inhibits several CDKs, including CDK5, which was shown to phosphorylate Rb$^{S807/811}$ to activate cell cycle progression [59].

The apparent decrease in E2F5/6 repressor mRNA levels can be consistent with the strong G1 arrest caused by dual pan-HDAC/CDK inhibition. First, our RNA-seq in HL-60 and U-937 cells shows that transcripts encoding repressors E2F5 and 6 decrease after treatment. At the same time, activators E2F1-3 are strongly downregulated. This indicates that the overall transcriptional activity of E2F-responsive genes is reduced. Moreover, despite reduced mRNA levels, E2F5 and E2F6 can be stabilized after translation when pocket proteins p130/p107 stay hypophosphorylated, a direct result of CDK inhibition. This results in the formation of repressive complexes like "Dimerization partner, RB-like, E2F, and MuvB" (DREAM), which maintain cells in quiescence. HDAC blockade further facilitates the assembly of these complexes by increasing acetylation-mediated chromatin accessibility at E2F-repressed promoters [60].

The primary function of E2F5 remains transcriptional repression. Therefore, it is conceivable that accumulation of E2F5/6 proteins, despite reduced mRNA levels, contributes to a compensatory mechanism reinforcing the cell cycle arrest caused by decreased E2F1-3 levels. Overall, these findings reconcile the increase in E2F repressor proteins with the observed cell cycle arrest and support previous reports that the coordinated downregulation of activator E2Fs and stabilization of

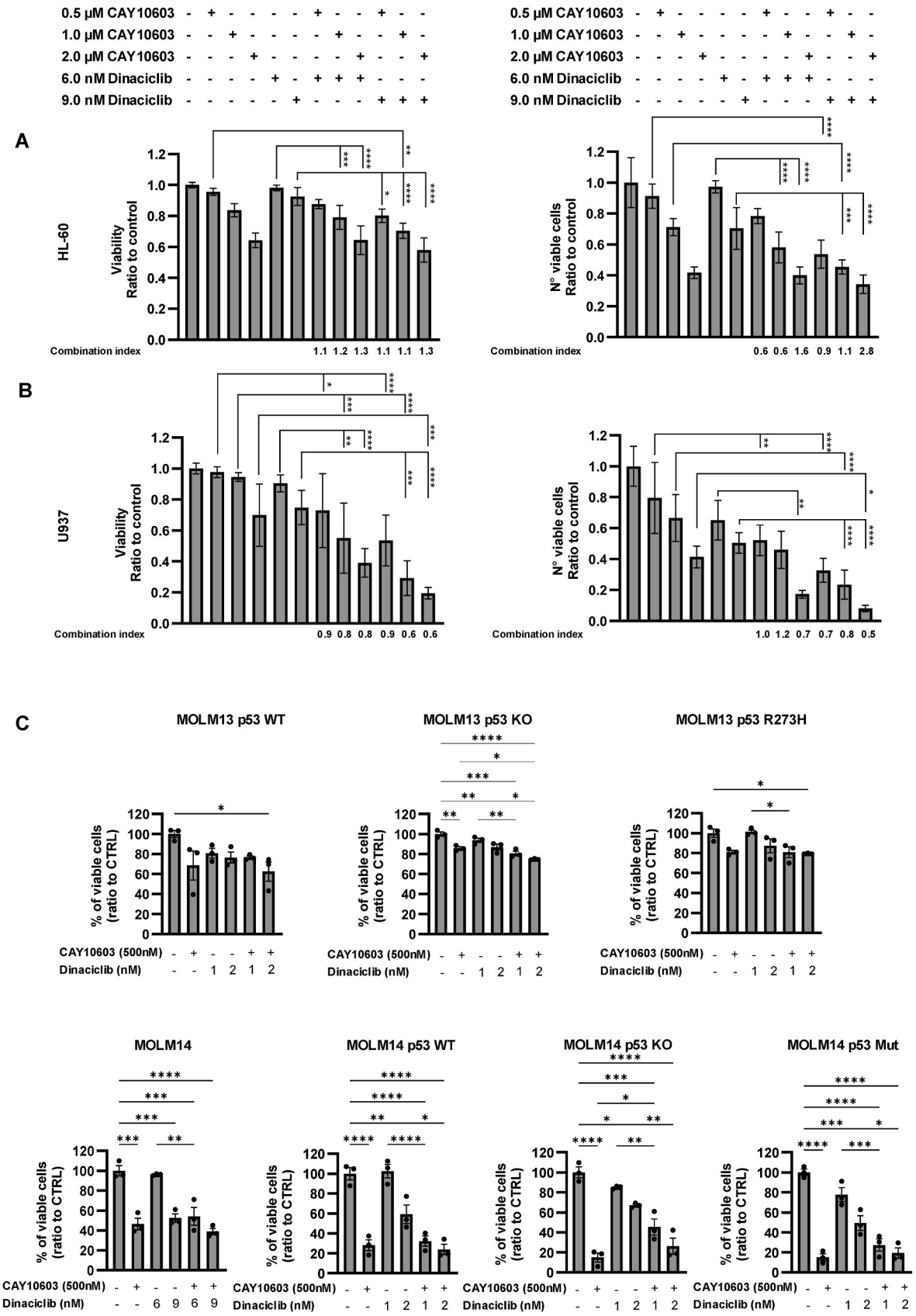

Fig. 7. Effect of CAY10603 and Dinaciclib combination on cell viability and clonogenic capacity. **A-B.** Cell viability assessment after 24 h of the indicated treatments with a combination of CAY10603 and dinaciclib in HL-60 (**A**) and U-937 (**B**) cell lines. **C.** Cell viability assessment after 24 h of the indicated treatments with a combination of CAY10603 and dinaciclib in MOLM-13 TP53 wild type, MOLM-13 TP53 KO, MOLM-13 TP53 mutant, MOLM-14, MOLM-14 TP53 wild type, MOLM-14 TP53 KO, and MOLM-14 TP53 mutant cell lines. Data represent the mean ± SD of at least 3 independent experiments. P values were determined by one-way ANOVA with Tukey's multiple comparison test. Significance levels are indicated as follows: *$p \leq 0.05$, **$p \leq 0.01$, ***$p \leq 0.001$, ****$p \leq 0.0001$.

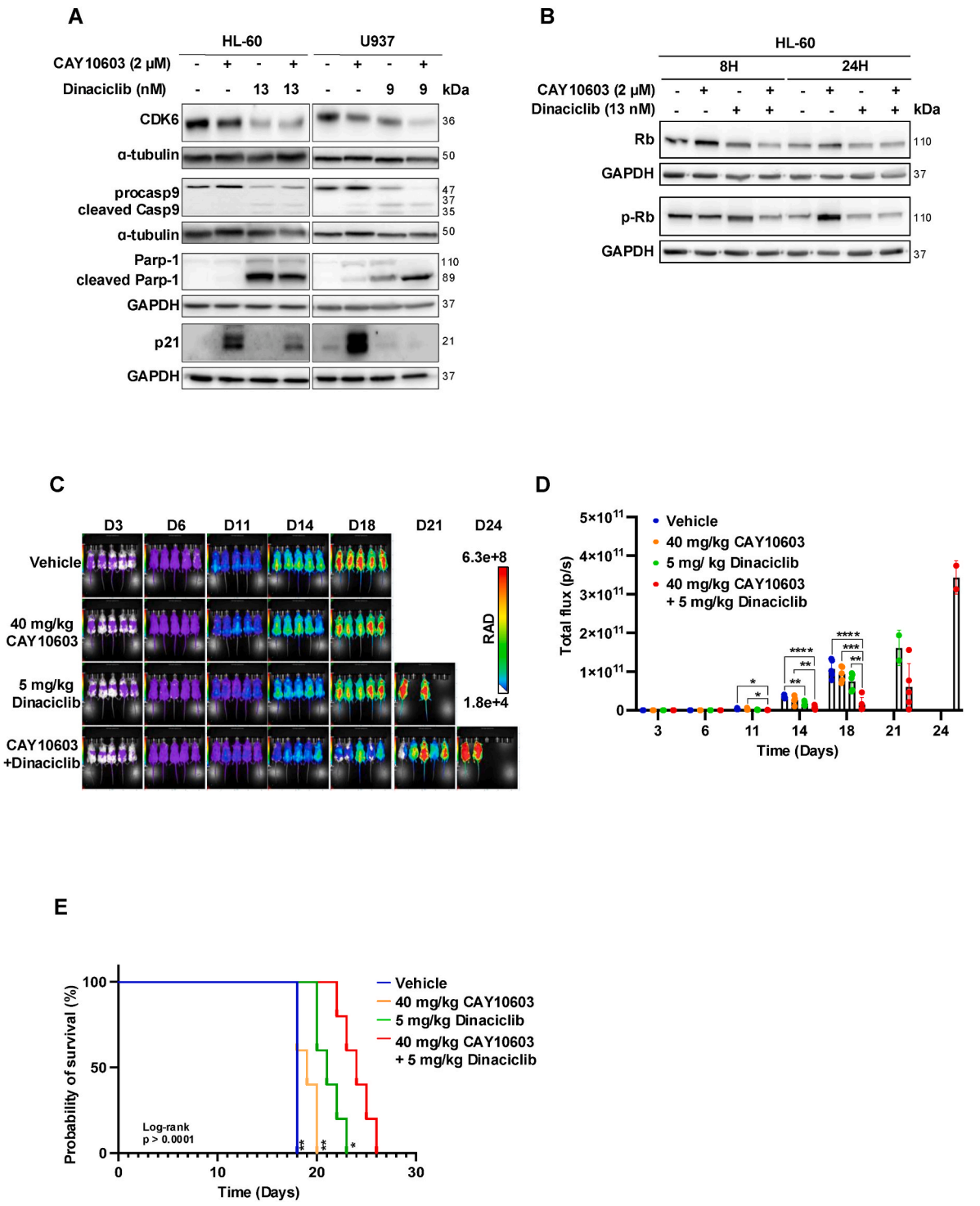

Fig. 8. Effect of CAY10603 and Dinaciclib combination on protein expression and in vivo survival. **A-B.** Western blot analysis of CDK6, procaspase-9, PARP-1, p21 (C), RB, and phosphorylated RB (D) following the indicated treatments. GAPDH and α-tubulin were used as internal loading controls. Immunoblot pictures represent at least three independent experiments. **C-E.** Synergistic effect of the combination of CAY10603 and dinaciclib in a U-937-Luc xenograft study (N = 5 mice/group). **C.** Bioluminescence imaging of U-937-Luc cells after tail vein injection. CAY10603 (40 mg/kg; intraperitoneal injection; 5 times a week) and dinaciclib (5 mg/kg; intraperitoneal injection; 3 times a week) were administered alone or in combination. N = 5 mice/group. **D.** Quantification of total bioluminescent flux over time. **E.** Kaplan-Meier survival analysis. Data are presented as mean ± SD (N = 5). P values were determined by one-way ANOVA with Tukey's multiple comparison test (**D**) and Log-Rank Test **(E)**. Significance levels are indicated as follows: *p ≤ 0.05, **p ≤ 0.01, ***p ≤ 0.001, ****p ≤ 0.0001. Blots are representative of three independent experiments.

repressor E2Fs are key features of effective anti-proliferative therapy [60].

Although HDACis are designed to block deacetylases, they also shift the acetylation balance by indirectly affecting the histone acetyltransferases (HATs) p300 and CBP. HDAC inhibition lifts the negative regulation that class I/II HDACs usually impose on p300 autoacetylation, momentarily increasing its catalytic activity [61]. Activated p300 is the main enzyme that adds lysine acetyl groups to proteins involved in cell cycle progression and apoptosis, especially TP53 [62].

The functional effect of TP53 acetylation varies greatly depending on the allele. As seen in our HL-60 model, acetylation of the missing lysines does not matter in cells with null or loss-of-function mutations, or complete gene silencing. Conversely, tumors with partially functional or "gain-of-function" (GOF) TP53 mutants can respond to increased acetyl-p53 in two ways: (i) restoring some tumor-suppressor activity, or (ii) activating alternative pro-apoptotic programs that are unique to the mutant protein [63]. GOF TP53 variants are rare in AML and mostly unstudied, but it is worth exploring whether HDACi could change their transcriptional output.

Beyond TP53, p300-mediated acetylation of MYC at K148 and K323 marks the oncoprotein for ubiquitin-dependent degradation and reduces its transactivation potential [64]. HDACi-driven activation of p300 thus converges with direct HDAC inhibition to suppress MYC and E2F signaling, an effect observed as a significant reduction of "MYC Targets" and decreased E2F1 expression in our RNA-seq data. These events shift the transcriptional balance toward CDK inhibitors like $p21^{WAF1}$ and $p15^{INK4B}$, strengthening cell-cycle arrest and priming cells for apoptosis. Future studies that measure p300 levels, catalytic activity, and site-specific TP53 acetylation in primary AML samples will help clarify how this HAT axis works with the HDAC/CDK blockade to produce the observed anti-leukemic effects.

The pronounced synergy observed *in vitro*, coupled with the significant reduction of the leukemic burden and extended survival in mice, underscores the potential of this combination for $AML^{TP53mut}$ patients. These findings have important clinical implications. The strong efficacy of dual CDK/HDAC inhibition supports further evaluation in clinical trials to determine safety, optimal dosing, and therapeutic efficacy in patients with $AML^{TP53mut}$. Moreover, incorporating TP53 mutation status and mutational burden into standard diagnostic and prognostic procedures could refine risk stratification and guide treatment decisions. Our analysis reinforces the adverse prognostic impact of the high TP53 clonal burden, measured by VAF (quartile values), on AML patient survival outcomes. While a median-based stratification did not discriminate outcomes, patients in the upper quartile of the VAF distribution showed significantly poorer survival. This is consistent with reports linking higher TP53 VAF to dominant leukemic clones with aggressive biology and chemoresistance. These findings are from exploratory thresholds; therefore, they should be validated in independent cohorts before being used clinically. Nonetheless, they emphasize the potential value of including quantitative TP53 mutation metrics, rather than just binary mutation status, in prognostic assessments.

It is crucial to recognize study limitations and consider potential off-target effects. Mechanistically, additional research is needed to clarify how HDACi restore CDKN1A/p21 and CDKN2B/p15 expression and to investigate resistance mechanisms against dual CDK/HDAC inhibition. Although we employed multiple $AML^{TP53mut}$ and AML^{TP53wt} cell lines, it is uncertain how widely these results will apply to the genetic and phenotypic diversity of human AML. The concentrations and treatment durations used in our study may not fully reflect the pharmacokinetics and pharmacodynamics observed in patients. Additionally, the study focused on cell-based assays validated by orthotopic xenograft models, which are informative but cannot fully represent the complexity of the tumor microenvironment and the immune system's role in AML progression and treatment response. Nevertheless, these observations suggest a promising therapeutic avenue for overcoming resistance and improving results in this difficult AML subgroup [44].

Previous studies have shown that HDACi can variably affect immune cell subsets [65]. Although HDACi like entinostat can enhance natural killer (NK) cell activity, they may paradoxically cause immune suppression by increasing inhibitory receptors [66]. HDACi impair $CD4^+$ T-cell function and promote regulatory T-cell (Treg) differentiation by suppressing cytokine expression and interleukin-6 receptor (IL-6R) signaling [67,68]. In our results, we observed a transient reduction in circulating lymphocytes, while monocyte levels recovered by days 6 and 14 after treatment with the combination of CAY10603 and dinaciclib in C57BL/6 mice. Importantly, this combination did not cause severe neutropenia, thrombocytopenia, or basopenia, and all hematologic parameters stayed within or close to the normal reference range. Our findings, therefore, suggest that the CAY10603 and dinaciclib combination therapy did not significantly impact steady-state hematopoiesis.

Yan et al. showed that standard chemotherapy enriches TP53-mutant sub-clones and that single-agent vorinostat prevents this outgrowth by inducing apoptosis in both $AML^{TP53mut}$ and AML^{TP53wt} cells [69]. Our work corroborates the value of HDAC blockade but extends it in three key respects: (i) CAY10603 inhibits class-I/II HDACs two-to three-fold more potently than vorinostat, producing deeper suppression of MYC- and E2F-driven transcription; (ii) the addition of the multi-target CDK inhibitor dinaciclib neutralizes the HDACi-induced up-regulation of CDK2 and accelerates loss of short-lived survival proteins such as MCL-1, yielding synergistic cytotoxicity and a survival benefit in an orthotopic xenograft; and (iii) our data demonstrate that this dual epigenetic-transcriptional hit is TP53-agnostic, suggesting broader applicability than the single-agent strategy explored by Yan et al. [69].

Taken together, our data identify CAY10603 as a bona-fide pan-HDAC inhibitor that, when paired with low-nanomolar dinaciclib, reprograms MYC/E2F transcription, restores p21, and drives caspase-dependent apoptosis, not only in TP53-wild-type AML but also in TP53-mutant and TP53-null subtypes, effectively erasing their therapeutic resistance and providing a single TP53-agnostic therapeutic approach.

CRediT authorship contribution statement

Aurélien Pottier: Writing – original draft, Methodology, Investigation. **Sujung Park:** Writing – original draft, Supervision, Methodology, Investigation. **Yejin Lee:** Methodology, Formal analysis. **Francesca Liccardo:** Methodology, Investigation, Formal analysis, Data curation. **Haeun Yang:** Methodology, Investigation. **Jeonghye Park:** Methodology, Investigation. **Anne Lorant:** Writing – original draft, Software, Resources, Methodology, Investigation, Formal analysis, Data curation, Conceptualization. **Michael Schnekenburger:** Writing – original draft, Methodology, Formal analysis, Data curation, Conceptualization. **Davide Brusa:** Methodology. **Vladimir Li:** Methodology, Data curation. **Sergio Valente:** Resources, Methodology. **Antonello Mai:** Resources, Methodology. **Sarah J. Skuli:** Resources, Methodology. **Martin Carroll:** Resources, Methodology. **Steffen Boettcher:** Resources, Methodology. **Jean-Emmanuel Sarry:** Resources, Methodology. **Claudia Cerella:** Writing – review & editing, Writing – original draft, Visualization, Validation, Supervision, Software, Resources, Methodology, Investigation, Formal analysis, Data curation, Conceptualization. **Franck Morceau:** Writing – review & editing, Writing – original draft, Validation, Supervision, Project administration, Methodology, Investigation, Formal analysis, Data curation, Conceptualization. **Marc Diederich:** Writing – review & editing, Writing – original draft, Validation, Supervision, Resources, Project administration, Methodology, Funding acquisition, Formal analysis, Data curation, Conceptualization.

Ethics approval

All animal experiments at Seoul National University, Seoul, South Korea, complied with the Institute of Animal Care and Use Committee (IACUC) guidelines. The IACUC Ethics Committee approved the study

protocols (SNU-220704-6-3 and SNU-241112-4).

Availability of data

The data supporting this study's findings are available from the corresponding author upon request. The RNA-seq data are available in the GEO database under GSE305560.

Declaration of generative AI and AI-assisted technologies in the writing process

During the preparation of this work, the author(s) used Grammarly.com and ChatGTP to improve language and readability. After using this tool/service, the author(s) reviewed and edited the content as needed and took full responsibility for the publication's content.

Funding

The authors thank the "Recherche Cancer et Sang" foundation, the "Recherches Scientifiques Luxembourg", the "Een Häerz fir kriibskrank Kanner", the Action LIONS "Vaincre le Cancer", and Télévie Luxembourg. CC acknowledges support from the "Fondation Gustave et Simone Prévot" (Geneva, Switzerland). The authors thank the National Research Foundation (NRF) [Grant Number 370C-20220066] and the Brain Korea (BK21) PLUS program. SJS acknowledges funding from NIH T32HL0439, NIH KL2TR001879, ASH RTAF, and ASCO YIA. Martin Carroll acknowledges funding from NIH/NCI U54CA283759 and Veterans Merit Award I01BX000918.

Declaration of competing interest

The authors declare that they have no known competing financial interests or personal relationships that could have appeared to influence the work reported in this paper.

Acknowledgments

Not applicable.

Appendix A. Supplementary data

Supplementary data to this article can be found online at https://doi.org/10.1016/j.canlet.2025.218011.

References

[1] M. Konopleva, G. Martinelli, N. Daver, C. Papayannidis, A. Wei, B. Higgins, et al., MDM2 inhibition: an important step forward in cancer therapy, Leukemia 34 (11) (2020) 2858–2874.
[2] M. Munisamy, N. Mukherjee, L. Thomas, A.T. Pham, A. Shakeri, Y. Zhao, et al., Therapeutic opportunities in cancer therapy: targeting the p53-MDM2/MDMX interactions, Am. J. Cancer Res. 11 (12) (2021) 5762–5781.
[3] A.W. Roberts, Therapeutic development and current uses of BCL-2 inhibition, Hematol. Am. Soc. Hematol. Educ. Prog. 2020 (1) (2020) 1–9.
[4] J. Wu, Y. Liang, Y. Tan, Y. Tang, H. Song, Z. Wang, et al., CDK9 inhibitors reactivate p53 by downregulating iASPP, Cell. Signal. 67 (2020) 109508.
[5] P. Menichini, P. Monti, A. Speciale, G. Cutrona, S. Matis, F. Fais, et al., Antitumor effects of PRIMA-1 and PRIMA-1(Met) (APR246) in hematological malignancies: still a mutant P53-dependent affair? Cells 10 (1) (2021).
[6] D.M. English, S.N. Lee, K.A. Sabat, I.M. Baker, T.K. Pham, M.O. Collins, et al., Rapid degradation of histone deacetylase 1 (HDAC1) reveals essential roles in both gene repression and active transcription, Nucleic Acids Res. 53 (4) (2025) gkae1223.
[7] T. Liang, F. Wang, R.M. Elhassan, Y. Cheng, X. Tang, W. Chen, et al., Targeting histone deacetylases for cancer therapy: trends and challenges, Acta Pharm. Sin. B 13 (6) (2023) 2425–2463.
[8] M.A. Loycano, K.J. Pienta, S.R. Amend, Temporal myc dynamics permit mitotic bypass, promoting polyploid phenotypes, Cancer Lett. 613 (2025) 217526.
[9] U.S. Baghel, P. Kriplani, N.M. Patel, M. Kaur, K. Sharma, M. Meghani, et al., Flavopiridol: a promising cyclin-dependent kinase inhibitor in cancer treatment, Naunyn-Schmiedebergs Arch Pharmacol 398 (4) (2025) 3489–3511.
[10] M.S. Squires, L. Cooke, V. Lock, W. Qi, E.J. Lewis, N.T. Thompson, et al., AT7519, a cyclin-dependent kinase inhibitor, exerts its effects by transcriptional inhibition in leukemia cell lines and patient samples, Mol. Cancer Therapeut. 9 (4) (2010) 920–928.
[11] G.P. Gregory, S. Kumar, D. Wang, D. Mahadevan, P. Walker, N. Wagner-Johnston, et al., Pembrolizumab plus dinaciclib in patients with hematologic malignancies: the phase 1b KEYNOTE-155 study, Blood Adv. 6 (4) (2022) 1232–1242.
[12] S.K. Kumar, B. LaPlant, W.J. Chng, J. Zonder, N. Callander, R. Fonseca, et al., Dinaciclib, a novel CDK inhibitor, demonstrates encouraging single-agent activity in patients with relapsed multiple myeloma, Blood 125 (3) (2015) 443–448.
[13] A. Marr, S. Karmahapatra, D. Corbin, Y. Asemelash, S. Sher, S.R. Mitchell, et al., The multi-CDK inhibitor dinaciclib shows synergistic activity with the BET inhibitor PLX51107 and reverses BET resistance through inhibition of canonical wnt signaling in acute myeloid leukemia (AML), Blood 140 (Supplement 1) (2022) 3075–3076.
[14] H. Pariury, J. Fandel, S. Bachl, K.K. Ang, S. Markossian, C.G. Wilson, et al., Venetoclax and dinaciclib elicit synergistic preclinical efficacy against hypodiploid acute lymphoblastic leukemia, Haematologica 108 (5) (2023) 1272–1283.
[15] S.A. Im, Y.S. Lu, A. Bardia, N. Harbeck, M. Colleoni, F. Franke, et al., Overall survival with ribociclib plus Endocrine therapy in breast cancer, N. Engl. J. Med. 381 (4) (2019) 307–316.
[16] S. Johnston, M. Martin, A. Di Leo, S.A. Im, A. Awada, T. Forrester, et al., MONARCH 3 final PFS: a randomized study of abemaciclib as initial therapy for advanced breast cancer, NPJ Breast Cancer 5 (2019) 5.
[17] G.W. Sledge Jr., M. Toi, P. Neven, J. Sohn, K. Inoue, X. Pivot, et al., The effect of abemaciclib plus Fulvestrant on overall survival in Hormone receptor-positive, ERBB2-negative breast cancer that progressed on Endocrine therapy-MONARCH 2: a randomized clinical trial, JAMA Oncol. 6 (1) (2020) 116–124.
[18] N.C. Turner, D.J. Slamon, J. Ro, I. Bondarenko, S.A. Im, N. Masuda, et al., Overall survival with palbociclib and Fulvestrant in advanced breast cancer, N. Engl. J. Med. 379 (20) (2018) 1926–1936.
[19] J.P. Ruff, A.L. Kretz, M. Kornmann, D. Henne-Bruns, J. Lemke, B. Traub, The novel, Orally Bioavailable CDK9 inhibitor atuveciclib sensitises Pancreatic cancer cells to TRAIL-induced cell death, Anticancer Res. 41 (12) (2021) 5973–5985.
[20] Y. Sixto-Lopez, M. Bello, R.A. Rodriguez-Fonseca, M.C. Rosales-Hernandez, M. Martinez-Archundia, J.A. Gomez-Vidal, et al., Searching the conformational complexity and binding properties of HDAC6 through docking and molecular dynamic simulations, J. Biomol. Struct. Dyn. 35 (13) (2017) 2794–2814.
[21] C. Cerella, S.R. Gajulapalli, A. Lorant, D. Gerard, F. Muller, Y. Lee, et al., ATP1A1/BCL2L1 predicts the response of myelomonocytic and monocytic acute myeloid leukemia to cardiac glycosides, Leukemia 38 (1) (2024) 67–81.
[22] M. Schnekenburger, A. Lorant, S.R. Gajulapalli, R. Rajora, J.Y. Lee, A. Mazumder, et al., Dual inhibition of sirtuins 1 and 2: reprogramming metabolic energy dynamics in chronic myeloid leukemia as an immunogenic anticancer strategy, Cancer Commun (Lond) 44 (8) (2024) 915–920.
[23] D. Bottomly, N. Long, A.R. Schultz, S.E. Kurtz, C.E. Tognon, K. Johnson, et al., Integrative analysis of drug response and clinical outcome in acute myeloid leukemia, Cancer Cell 40 (8) (2022) 850–864 e859.
[24] I. Baccelli, Y. Gareau, B. Lehnertz, S. Gingras, J.F. Spinella, S. Corneau, et al., Mubritinib targets the electron Transport Chain complex I and reveals the landscape of OXPHOS dependency in acute myeloid leukemia, Cancer Cell 36 (1) (2019) 84–99 e88.
[25] G. Ehx, J.D. Larouche, C. Durette, J.P. Laverdure, L. Hesnard, K. Vincent, et al., Atypical acute myeloid leukemia-specific transcripts generate shared and immunogenic MHC class-I-associated epitopes, Immunity 54 (4) (2021) 737–752 e710.
[26] V.P. Lavallee, J. Chagraoui, T. MacRae, M. Marquis, A. Bonnefoy, J. Krosl, et al., Transcriptomic landscape of acute promyelocytic leukemia reveals aberrant surface expression of the platelet aggregation agonist Podoplanin, Leukemia 32 (6) (2018) 1349–1357.
[27] A. Maiga, S. Lemieux, C. Pabst, V.P. Lavallee, M. Bouvier, G. Sauvageau, et al., Transcriptome analysis of G protein-coupled receptors in distinct genetic subgroups of acute myeloid leukemia: identification of potential disease-specific targets, Blood Cancer J. 6 (6) (2016) e431.
[28] M. Marquis, C. Beaubois, V.P. Lavallee, M. Abrahamowicz, C. Danieli, S. Lemieux, et al., High expression of HMGA2 independently predicts poor clinical outcomes in acute myeloid leukemia, Blood Cancer J. 8 (8) (2018) 68.
[29] D.P. Nusinow, J. Szpyt, M. Ghandi, C.M. Rose, E.R. McDonald 3rd, M. Kalocsay, et al., Quantitative proteomics of the cancer cell line Encyclopedia, Cell 180 (2) (2020) 387–402 e316.
[30] F. Marchi, V.M. Shastri, R.J. Marrero, N.H.K. Nguyen, A. Ottl, A.K. Schade, et al., Epigenomic diagnosis and prognosis of acute myeloid leukemia, Nat. Commun. 16 (1) (2025) 6961.
[31] J.S. Welch, A.A. Petti, C.A. Miller, C.C. Fronick, M. O'Laughlin, R.S. Fulton, et al., TP53 and decitabine in acute myeloid leukemia and myelodysplastic syndromes, N. Engl. J. Med. 375 (21) (2016) 2023–2036.
[32] N. Daver, J. Senapati, A. Maiti, S. Loghavi, T.M. Kadia, C.D. DiNardo, et al., Phase I/II study of azacitidine (AZA) with venetoclax (VEN) and magrolimab (Magro) in patients (pts) with newly diagnosed (ND) Older/Unfit or high-risk acute myeloid leukemia (AML) and relapsed/refractory (R/R) AML, Blood 140 (Supplement 1) (2022) 141–144.
[33] N.G. Daver, P. Vyas, S. Kambhampati, M.M. Al Malki, R.A. Larson, A.S. Asch, et al., Tolerability and efficacy of the Anticluster of differentiation 47 antibody magrolimab combined with azacitidine in patients with previously untreated AML: phase Ib results, J. Clin. Oncol. 41 (31) (2023) 4893–4904.

[34] A.M. Brunner, J. Esteve, K. Porkka, S. Knapper, E. Traer, S. Scholl, et al., Phase Ib study of sabatolimab (MBG453), a novel immunotherapy targeting TIM-3 antibody, in combination with decitabine or azacitidine in high- or very high-risk myelodysplastic syndromes, Am. J. Hematol. 99 (2) (2024) E32–E36.
[35] A.M. Zeidan, J. Westermann, T. Kovacsovics, S. Assouline, A.C. Schuh, H.-J. Kim, et al., AML-484 first results of a phase II study (STIMULUS-AML1) investigating sabatolimab + azacitidine + venetoclax in patients with newly diagnosed acute myeloid leukemia (ND AML), Clin. Lymphoma Myeloma Leuk. 22 (2022) S255.
[36] N. Daver, G. Garcia-Manero, S. Basu, P.C. Boddu, M. Alfayez, J.E. Cortes, et al., Efficacy, safety, and Biomarkers of response to azacitidine and nivolumab in relapsed/refractory acute myeloid leukemia: a Nonrandomized, open-label, phase II study, Cancer Discov. 9 (3) (2019) 370–383.
[37] T. Cluzeau, M. Sebert, R. Rahme, S. Cuzzubbo, J. Lehmann-Che, I. Madelaine, et al., Eprenetapopt Plus Azacitidine in TP53-Mutated Myelodysplastic Syndromes and Acute Myeloid Leukemia: A Phase II Study by the Groupe Francophone des Myelodysplasies (GFM), J. Clin. Oncol. 39 (14) (2021) 1575–1583.
[38] G.L. Uy, I. Aldoss, M.C. Foster, P.H. Sayre, M.J. Wieduwilt, A.S. Advani, et al., Flotetuzumab as salvage immunotherapy for refractory acute myeloid leukemia, Blood 137 (6) (2021) 751–762.
[39] T. Kobayashi, T. Makino, K. Yamashita, T. Saito, K. Tanaka, T. Takahashi, et al., APR-246 induces apoptosis and enhances chemo-sensitivity via activation of ROS and TAp73-Noxa signal in oesophageal squamous cell cancer with TP53 missense mutation, Br. J. Cancer 125 (11) (2021) 1523–1532.
[40] L.A. Donehower, T. Soussi, A. Korkut, Y. Liu, A. Schultz, M. Cardenas, et al., Integrated analysis of TP53 gene and pathway alterations in the cancer genome atlas, Cell Rep. 28 (5) (2019) 1370–1384 e1375.
[41] J. Tian, M. Han, F. Song, Y. Liu, Y. Shen, J. Zhong, Advances of HDAC inhibitors in tumor therapy: potential applications through immune modulation, Front. Oncol. 15 (2025) 1576781.
[42] A. Baker, G.P. Gregory, I. Verbrugge, L. Kats, J.J. Hilton, E. Vidacs, et al., The CDK9 inhibitor dinaciclib exerts potent apoptotic and Antitumor effects in preclinical models of MLL-rearranged acute myeloid leukemia, Cancer Res. 76 (5) (2016) 1158–1169.
[43] S. Al Bitar, H. Gali-Muhtasib, The role of the cyclin dependent kinase inhibitor p21 (cip1/waf1) in targeting cancer: molecular mechanisms and novel therapeutics, Cancers (Basel) 11 (10) (2019).
[44] M.C. Sachweh, C.J. Drummond, M. Higgins, J. Campbell, S. Lain, Incompatible effects of p53 and HDAC inhibition on p21 expression and cell cycle progression, Cell Death Dis. 4 (3) (2013) e533.
[45] G. Song, B.C. Valdez, Y. Li, J.R. Dominguez, P. Corn, R.E. Champlin, et al., The histone deacetylase inhibitor SAHA sensitizes acute myeloid leukemia cells to a combination of nucleoside analogs and the DNA-alkylating agent busulfan, Leuk. Lymphoma 55 (7) (2014) 1625–1634.
[46] S. Kim, J. Armand, A. Safonov, M. Zhang, R.K. Soni, G. Schwartz, et al., Sequential activation of E2F via Rb degradation and c-Myc drives resistance to CDK4/6 inhibitors in breast cancer, Cell Rep. 42 (11) (2023) 113198.
[47] Y. Liu, Z. Su, O. Tavana, W. Gu, Understanding the complexity of p53 in a new era of tumor suppression, Cancer Cell 42 (6) (2024) 946–967.
[48] L. Garcia-Gutierrez, M.D. Delgado, J. Leon, MYC oncogene contributions to release of cell cycle brakes, Genes (Basel) 10 (3) (2019) 244.
[49] T.Z. Zeleke, Q. Pan, C. Chiuzan, M. Onishi, Y. Li, H. Tan, et al., Network-based assessment of HDAC6 activity predicts preclinical and clinical responses to the HDAC6 inhibitor ricolinostat in breast cancer, Nat. Cancer 4 (2) (2023) 257–275.
[50] A. Saidahmatov, J. Li, S. Xu, X. Hu, X. Gao, W. Kan, et al., Discovery of novel 2-Aminopyridine-based and 2-Aminopyrimidine-based derivatives as potent CDK/HDAC dual inhibitors for the treatment of refractory Solid tumors and hematological malignancies, J. Med. Chem. 67 (17) (2024) 15220–15245.
[51] F. Faiola, X. Liu, S. Lo, S. Pan, K. Zhang, E. Lymar, et al., Dual regulation of c-Myc by p300 via acetylation-dependent control of Myc protein turnover and coactivation of Myc-induced transcription, Mol. Cell Biol. 25 (23) (2005) 10220–10234.
[52] A. Nebbioso, V. Carafa, M. Conte, F.P. Tambaro, C. Abbondanza, J. Martens, et al., c-Myc modulation and acetylation is a key HDAC inhibitor target in cancer, Clin. Cancer Res. 23 (10) (2017) 2542–2555.
[53] M. Hurd, J. Pino, K. Jang, M.M. Allevato, M. Vorontchikhina, W. Ichikawa, et al., MYC acetylated lysine residues drive oncogenic cell transformation and regulate select genetic programs for cell adhesion-independent growth and survival, Genes Dev. 37 (19–20) (2023) 865–882.
[54] S.D. Cappell, M. Chung, A. Jaimovich, S.L. Spencer, T. Meyer, Irreversible APC (Cdh1) inactivation underlies the point of No return for cell-cycle entry, Cell 166 (1) (2016) 167–180.
[55] B.Z. Carter, P.Y. Mak, W. Tao, E. Ayoub, L.B. Ostermann, X. Huang, et al., Combined inhibition of BCL-2 and MCL-1 overcomes BAX deficiency-mediated resistance of TP53-mutant acute myeloid leukemia to individual BH3 mimetics, Blood Cancer J. 13 (1) (2023) 57.
[56] M. Chung, C. Liu, H.W. Yang, M.S. Koberlin, S.D. Cappell, T. Meyer, Transient hysteresis in CDK4/6 activity underlies passage of the restriction point in G1, Mol. Cell 76 (4) (2019) 562–573 e564.
[57] H.W. Yang, M. Chung, T. Kudo, T. Meyer, Competing memories of mitogen and p53 signalling control cell-cycle entry, Nature 549 (7672) (2017) 404–408.
[58] I. Pellarin, A. Dall'Acqua, A. Favero, I. Segatto, V. Rossi, N. Crestan, et al., Cyclin-dependent protein kinases and cell cycle regulation in biology and disease, Signal Transduct. Targeted Ther. 10 (1) (2025) 11.
[59] S. Batra, S. Jahan, A. Ashraf, B. Alharby, T. Jawaid, A. Islam, et al., A review on cyclin-dependent kinase 5: an emerging drug target for neurodegenerative diseases, Int. J. Biol. Macromol. 230 (2023) 123259.
[60] M. Sun, Y. Ji, G. Zhang, Y. Li, F. Dong, T. Wu, Posttranslational modifications of E2F family members in the physiological state and in cancer: roles, mechanisms and therapeutic targets, Biomed. Pharmacother. 178 (2024) 117147.
[61] D.P. Stiehl, D.M. Fath, D. Liang, Y. Jiang, N. Sang, Histone deacetylase inhibitors synergize p300 autoacetylation that regulates its transactivation activity and complex formation, Cancer Res. 67 (5) (2007) 2256–2264.
[62] P. Gou, W. Zhang, Protein lysine acetyltransferase CBP/p300: a promising target for small molecules in cancer treatment, Biomed. Pharmacother. 171 (2024) 116130.
[63] L.J. Hernandez Borrero, W.S. El-Deiry, Tumor suppressor p53: biology, signaling pathways, and therapeutic targeting, Biochim. Biophys. Acta Rev. Canc 1876 (1) (2021) 188556.
[64] J. Chen, S. Zhang, X. Huang, Q. Wang, W. Xu, J. Huang, et al., Sialylated IgG-activated integrin beta4-Src-Erk axis stabilizes c-Myc in a p300 lysine acetyltransferase-dependent manner to promote colorectal cancer liver metastasis, Neoplasia 61 (2025) 101140.
[65] B. Moran, M. Davern, J.V. Reynolds, N.E. Donlon, J. Lysaght, The impact of histone deacetylase inhibitors on immune cells and implications for cancer therapy, Cancer Lett. 559 (2023) 216121.
[66] J.M. Idso, S. Lao, N.J. Schloemer, J. Knipstein, R. Burns, M.S. Thakar, et al., Entinostat augments NK cell functions via epigenetic upregulation of IFIT1-STING-STAT4 pathway, Oncotarget 11 (20) (2020) 1799–1815.
[67] R. Glauben, E. Sonnenberg, M. Wetzel, P. Mascagni, B. Siegmund, Histone deacetylase inhibitors modulate interleukin 6-dependent CD4+ T cell polarization in vitro and in vivo, J. Biol. Chem. 289 (9) (2014) 6142–6151.
[68] M. Pace, J. Williams, A. Kurioka, A.B. Gerry, B. Jakobsen, P. Klenerman, et al., Histone deacetylase inhibitors enhance CD4 T cell susceptibility to NK cell killing but reduce NK cell function, PLoS Pathog. 12 (8) (2016) e1005782.
[69] B. Yan, D. Claxton, S. Huang, Y. Qiu, AML chemoresistance: the role of mutant TP53 subclonal expansion and therapy strategy, Exp. Hematol. 87 (2020) 13–19.